NASA CR-168287

ADVANCED SMOKE METER DEVELOPMENT:

SURVEY AND ANALYSIS

by

R. W. Pitz, C. M. Penney, C. M. Stanforth, and W. M. Shaffernocker

General Electric Company
Corporate Research and Development
Schenectady, New York 12301

and

General Electric Company
Aircraft Engine Business Group
Advanced Technology Programs Department
Cincinnati, Ohio 45215

Prepared for

National Aeronautics and Space Administration
Lewis Research Center
21000 Brookpark Road
Cleveland, Ohio 44135

CONTRACT NAS3-23532

NASA

NASA CR-168287

ADVANCED SMOKE METER DEVELOPMENT:

SURVEY AND ANALYSIS

by

R. W. Pitz, C. M. Penney, C. M. Stanforth, and W. M. Shaffernocker

General Electric Company
Corporate Research and Development
Schenectady, New York 12301

and

General Electric Company
Aircraft Engine Business Group
Advanced Technology Programs Department
Cincinnati, Ohio 45215

Prepared for

National Aeronautics and Space Administration
Lewis Research Center
21000 Brookpark Road
Cleveland, Ohio 44135

CONTRACT NAS3-23532

TABLE OF CONTENTS

Section		Page
	Nomenclature	v
	Summary	(1)
1	Introduction	2
2	Identification and Ranking of Measurement Techniques	3
3	Analysis of Promising Concepts	4
	3.1 Light Scattering	4
	3.1.1 Photometric Light Scattering Particle Measurements	4
	3.1.2 Particle Counters	5
	3.2 Direct Transmission	7
	3.3 Modulated Transmission (MODTRAN)	8
	3.3.1 General Description	8
	3.3.2 Theoretical Principles	9
	3.3.3 Modulated Transmission Proof of Principle Experiment	11
	3.3.4 Potential Problems	13
	3.3.5 Summary	14
	3.4 Crossed Beam Absorption Counter (CBAC)	15
	3.4.1 General Description	15
	3.4.2 Theoretical Principles	15
	3.4.3 Potential Problems	20
	3.4.4 Summary	20
	3.5 Tapered Element Oscillating Microbalance (TEOM)	23
	3.5.1 General Description	23
	3.5.2 Theoretical Principles	23
	3.5.3 Potential Problems	25
	3.5.4 Summary	25
	3.6 Laser Induced Incandescence (LIN)	27
	3.6.1 General Description	27
	3.6.2 Theoretical Principles	27
	3.6.3 Potential Problems	30
	3.6.4 Summary	30
	3.7 Photoacoustic Spectroscopy (PAS)	31
	3.7.1 General Description	33
	3.7.2 Theoretical Principles	33
	3.7.3 Potential Problems	35
	3.7.4 Summary	37
4	Recommendations for Future Work	39
5	Summary and Conclusions	41

TABLE OF CONTENTS (Cont'd)

Section		Page
	Appendix	43
	References	44

Nomenclature

a_e	Average fractional light extinction
a_o	Laser beam cross sectional area (m^2)
A_A	Specific absorption coefficient (m^2/g)
A_E	Specific extinction coefficient (m^2/g)
b_A	Absorption coefficient (m^{-1})
b_E	Extinction coefficient (m^{-1})
B_o	Signal bandwidth (Hz)
B_λ	Planck radiation function
c	Speed of light (m/s)
C	Gas concentration
C_c	Specific heat of carbon
C_g	Specific heat of the gas
C_p	Specific heat at constant pressure
C_v	Specific heat at constant volume
d	Particle diameter (μm)
d_{ave}	Average soot diameter (μm)
d_f	Fringe spacing (μm)
d_o	Laser beam waist (m)
D	Cell diameter (m)
D_o	Probe volume depth (m)
f	Taper element vibration frequency (Hz)
f_o	Chopping frequency (Hz)
$F(r)$	Particle size distribution (m^{-1})
g	TEOM mass resolution (g)
h	Planck's constant
H	Probe height (m)
I	Transmitted light power (watts)
I_a	Original light power of source per unit area ($watts/cm^2$)
I_c	Laser irradiance on the centerline of the beam ($watts/cm^2$)
I_D	Power of incandescence (watts)
I_e	Spectral radiance of incandescent emission ($watts/cm^2$-nm-sr)
I_l	Integrated laser power (watts)

I_N	Transmitted light power through optical elements (watts)
I_o	Original light power of source (watts)
I_r	Laser irradiance at a radius of r_o (watts/cm^2)
I_s	Scattered light power (watts)
k	Boltzmann constant (J/K)
k_s	Scattering constant
K	Force constant (kg/sec^2)
K_o	Effective force constant (kg/sec^2)
K_s	Scattering constant
L	Optical path length
m	Complex index of refraction
m_e	Effective mass (g)
m_f	Filter element mass (g)
m_o	Tapered element mass (g)
m_p	Particulate mass (g)
M	Molecular weight (g/mole)
N	Number density of particles (m^{-3})
N_A	Avogadro's number (mole^{-1})
N_{max}	Maximum number density of particles (m^{-3})
N_{ph}	Number of detected photons
P	Gas pressure (Pa)
P_e	Equilibrium pressure fluctuations (Pa)
q	Quantum efficiency
Q	Cell quality
r	Particle radius (μm)
r_{min}	Minimum particle radius (μm)
R	Cell responsivity (mv-m/w)
R_{res}	Cell responsivity at resonance (mv-m/w)
S	Acoustic signal (rms volts)
S_I	Incandescence signal (Joules)
t	Time (sec)
t_o	Particle transit time (sec)
T_w	Average transmission of the optical elements

u_p	Soot particle velocity (m/s)
V	Volume of the cell (m^3)

Greek Letters

α	Beam crossing angle
γ	Ratio of specific heats
δ	Length of probe volume
ϵ	Transmission of optics
θ	Particle temperature (K)
θ_0	Gas temperature (K)
λ	Wavelength (nm)
ρ	Soot concentration (mg/m^3)
ρ_a	Density of absorbing gas (kg/m^3)
ρ_{ave}	Average soot mass concentration (mg/m^3)
ρ_c	Solid density of carbon in soot (g/cm^3)
ρ_g	Gas density (kg/m^3)
ρ_{max}	Maximum soot mass concentration (mg/m^3)
ρ_{min}	Minimum soot mass concentration (mg/m^3)
σ_a	Absorption cross section (cm^2)
σ_e	Extinction cross section (cm^2)
σ_m	Microphone sensitivity (mV/Pa)
σ_N	Standard deviation of N samples
ϕ	Filter flowrate (ml/s)
Ω	Solid angle of collection optics (sr)
ω	Angular frequency (sec^{-1})

Subscripts

rms	Root mean square value of a variable

Superscripts

$'$	Fluctuating value of a variable

SUMMARY

Rapid response smoke meters with improved range, sensitivity, and accuracy are needed to measure the wide range of smoke emission levels produced by modern commercial and military jet engines. In this report, ideal smoke meter characteristics are determined to provide a basis for evaluation of candidate systems. After an examination of a wide range of smoke meter concepts, five promising techniques are analyzed in detail to evaluate compliance with the practical smoke meter requirements. Four of the smoke measurement concepts are optical methods: Modulated Transmission (MODTRAN), Cross Beam Absorption Counter (CBAC), Laser Induced Incandescence (LIN), and Photoacoustic Spectroscopy (PAS). A rapid response filter instrument called a Taper Element Oscillating Microbalance (TEOM) is also evaluated.

For each technique, the theoretical principles are described, the expected performance is determined, and the advantages and disadvantages are discussed. The expected performance is evaluated against each of the smoke meter specifications, and the key questions for further study are given. The most promising smoke meter technique analyzed was MODTRAN, which is a variation on a direct transmission measurement. The soot-laden gas is passed through a transmission cell, and the gas pressure is modulated by a speaker. MODTRAN measures only the fluctuating component of the light transmission that is directly proportional to the light extinction and is insensitive to window contamination. Light extinction from soot well below 1% can be measured. MODTRAN has the potential of meeting all the requirements of a practical jet engine smoke meter including dynamic range (1-100 mg/m^3), time response (1 per sec), and operation in a severe test cell environment. Recommendations are made for experiments to evaluate MODTRAN's performance and to answer critical questions in the development of MODTRAN and one other promising technique (LIN). These experiments would use the TEOM instrument as an auxiliary standard and thereby evaluate its performance.

Section 1

INTRODUCTION

Smoke emissions from jet aircraft first became a concern in the early 1960s because of the detectability of black smoke trails from military aircraft. Later, smoke emissions from commercial jet aircraft traffic near metropolitan airports, particularly during landings and takeoffs, were the object of studies assessing aircraft contributions to air pollution.[1] These problems are an ongoing concern and cause low smoke emissions to be a primary goal of the engine designer. Finally, interest in the use of broader specification aircraft fuels has led to concern over the increased smoke emissions from many of these fuels and the subsequently higher radiative loading of the combustor liner.

Efforts to control and reduce smoke emissions through new engine design and control technology are a continuing pursuit. These investigations have focused on both combustor design[2] and fuel additives[3] to reduce smoke emissions. Such efforts require accurate measurements to quantify smoke levels from jet engine exhausts. Smoke meters in current use are based on filtering techniques[4,5] which yield only long-term averages. These techniques require lengthy and costly engine tests, and the data reduction for them may take days to complete. Methods are needed with increased range, improved accuracy, and faster response.

With the recent advances in optical and laser measurements, alternate methods are starting to emerge for measurement of smoke levels. Laser-induced photoacoustic spectroscopy has been used to make measurements of soot from diesel exhausts.[6,7] Although diesel exhausts generally have higher smoke levels than those encountered in jet engines, optical techniques such as photoacoustic spectroscopy are promising candidates for accurate, rapid, and sensitive measurement of smoke from jet engines.

In view of these recent advances, this study was undertaken to survey and analyze current measurement technology for application to jet engine smoke measurement. A set of criteria for an ideal smoke meter was determined, and candidate systems from a wide range of sources were evaluated against these criteria to determine the most promising techniques. Five of the most promising techniques were analyzed in detail to determine their expected performance and compliance with practical smoke meter requirements.

Section 2

IDENTIFICATION AND RANKING OF MEASUREMENT TECHNIQUES

As a first step in the survey and analysis of advanced smoke measurement systems, a list of concepts deemed applicable to the practical and rapid measurement of smoke emissions from jet engines was identified. The list of concepts was generated by a thorough investigation of the state of the art of smoke and particle measurement technology. The investigation to prepare this list included literature and patent searches, consultation with experts, and a survey of available commercial products.

A set of criteria for an ideal smoke meter called General Smoke Meter Requirements was determined and is given in the Appendix. A preliminary analysis of each concept was carried out to determine its capability to satisfy these system specifications. Many instruments and concepts were judged unacceptable and were not entered in the list of candidates. Several of the concepts were based upon light transmission, but were rejected because of only marginal resolution at the low concentration of smoke defined in the system specification. Many of the concepts that depend upon the accumulation of particles and particle separation were eliminated because they required sampling times that were too long (much greater than 1 second). Also rejected were some concepts based on light scattering that could not make measurements of particles in the very small particle size range of jet engine smoke.

Five smoke measurement concepts were chosen as subjects for complete analysis. Four of the five concepts selected involve scattering and/or absorption of light. The following analysis section summarizes the advantages and disadvantages of each technique.

Section 3

ANALYSIS OF PROMISING CONCEPTS

In this section, we present initial analysis of the five highest ranked measurement concepts, including one commercial instrument (TEOM). Initially we discuss several standard light scattering techniques and direct transmission that are unacceptable as ultimate concepts but provide a basis for discussion of the more promising techniques.

3.1 LIGHT SCATTERING

There are two outstanding features of light scattering for particle measurements: sensitivity to very low concentrations and ability to handle wide concentration ranges. These advantages have been realized in numerous commercially available instruments. The major difficulty is a complicated, and often somewhat uncertain, relationship between the measured properties of the scattered light and the properties of the scattering particles. Efforts to reduce this uncertainty have led, for example, to a variety of measurement concepts, using different combinations of angle, wavelength, and polarization characteristics of the scattered light. The scattering concepts we have selected for analysis can be classified as photometric and particle counting.

3.1.1 Photometric Light Scattering Particle Measurements

Photometric measurements are based on the average intensity of light scattered from a collection of particles. A single measurement of intensity may be used, but often several measurements at different angles, wavelengths, and/or polarizations are obtained to provide more information about the particle distribution. The distinguishing characteristic of photometric measurements is that there are numerous particles in the measurement volume simultaneously instead of only one. For nominally spherical particles whose radii r are smaller than 0.1 μm, which is the range of major concern for "young" soot measurements, the light scattering per particle is proportional to r^6. Thus, if $F(r)$ represents the particle size distribution such that

$$\int_0^\infty F(r)\, dr = 1 \tag{3.1-1}$$

the light power scattered into a detector from a collection of particles in the beam is given by

$$I_s \simeq \delta \Omega \epsilon I_0 \int_0^{0.1\,\mu m} N (K_s/\lambda^4) r^6 F(r)\, dr \tag{3.1-2}$$

where I_0 is the incident beam power (watts), δ is the observed length of the incident beam, Ω is the observed solid angle, ϵ is the transmission of the receiving optics, N is the number density of particles in the beam, and K_s/λ^4 contains the optical and particle characteristics of the light scattering.

Since, in this particle size range, scattering measures the distribution-weighted average of r^6, while the mass is represented by the distribution-weighted average of r^3, light scattering does not provide a direct measure of mass concentration. Furthermore, in this range, the angle and polarization-dependent properties of the scattering do not provide convenient access to information about the size distribution. Therefore, in order to use photometric light scattering to measure particle mass concentration, one must have considerable information about the size distribution from other sources.

3.1.2 Particle Counters

Particle counters measure the scattered light from single particles passing through the focal volume of a light source. The particle diameter is determined from the intensity of the burst of scattered light as the particle passes through the beam. The frequency of particle counts is measured and the particle velocity is determined by passing the particle-laden gas through a cell at a known velocity. Assuming a density for the soot particles ($\approx$ 2 g/cc), the mass loading of the particulate can be determined.

Particle counters observe particles one at a time by reducing the active volume until the probability that it will contain more than one observable particle at any time is very small. The minimum active volume is limited to about 10^{-9} cm^3 by the wave nature of light, and practical alignment considerations. Therefore, the maximum allowable density for accurate counting measurements is on the order of 10^8 particles per cubic centimeter, and practical difficulties become substantial for densities much above 10^6 particles/cm^3.

We can now estimate the minimum detectable size of a soot particle from a particle counter. For laser light scattered from a particle in the Rayleigh regime ($r < 0.1\ \mu$m for $\lambda = 500$ nm), the scattered light measured in a plane perpendicular to the plane of polarization of the incident light is,[8]

$$I_s = \epsilon\Omega \frac{I_0}{a_0} \frac{r^6}{\lambda^4} 16\pi^4 \left| \frac{m^2-1}{m^2+2} \right|^2 \tag{3.1-3}$$

where I_s is the detected power (watts) of scattered light from a laser beam of power, I_0, and a cross sectional area, a_0. The collection optics has an efficiency, ϵ, and collects light at a solid angle, Ω. The effective complex index of refraction of the soot particles is m.

The number of photons detected will be

$$N_{ph} = \frac{d_0}{u_p} \frac{qI_s}{(hc/\lambda)} \tag{3.1-4}$$

where d_0/u_p is the transit time of the particle through the beam, and (hc/λ) is the energy of a photon of light. Here d_0 is the beam diameter at the probe volume, u_p is the velocity perpendicular to the laser beam, h is Planck's constant, c is the speed of light, and q is the quantum efficiency of the detector.

From the two equations above, one can solve for the radius of the particle.

$$r = \left[\frac{a_0 u_p}{I_0 d_0} \frac{\lambda^4 (hc/\lambda) N_{ph}}{q\epsilon\Omega k_s} \right]^{\frac{1}{6}} \tag{3.1-5}$$

where

$$k_s = 16\pi^4 \left| \frac{m^2-1}{m^2+2} \right|^2 \tag{3.1-6}$$

In order to prevent carbon particle vaporization (see Section 3.6 on LIN) the light power density must be limited by the condition

$$\frac{I_0 d_0}{a_0 u_p} \leqslant 0.1 \text{ J/cm}^2 \tag{3.1-7}$$

In our calculations, we will use 0.1 J/cm^2.

If all the particles have the same radius, r, then to measure the soot mass concentration to 10% accuracy, one must determine r^3 to 10% accuracy. Since $r^3 \approx N_{ph}^{1/2}$ a 20% uncertainty in N_{ph} will give rise to a 10% uncertainty in r^3 (see Kline and McClintock[9]). According to the Poisson statistics of a photodetector, the standard deviation of N_{ph} photons is,

$$\sigma_N = \sqrt{N_{ph}} \quad . \tag{3.1-8}$$

Thus to measure N_{ph} to 20% accuracy, where the uncertainty limits are defined as $\pm \sigma_N$, one needs to obtain $N_{ph} = 25$ photons.

The solid angle for light collection must be small enough to only collect light from a constant intensity region in the beam ($\Omega = w/g$ 0.1 *sr*). The other representative values for the optical system are:

$$\epsilon = 0.2$$

$$q = 0.2$$

$$\lambda = 500 \ nm$$

and the soot complex index of refraction is,[10]

$$m = 1.6 - 0.6i$$

giving,

$$k = 377.$$

Now the minimum radius for a mass measurement to 10% accuracy is (Eq. 3.1-5),

$$r_{min} = 0.03 \ \mu m \ .$$

Equation (3.1-5) indicates that r_{min} depends only weakly on the various optical parameters. A factor of 64 improvement in optical efficiency will only lower the minimum radius by a factor of 2. Particle counters do not appear to provide a good approach to soot concentration measurements since there will often be a concern that a significant portion of the soot mass will be in particles with radii smaller than 0.03 μm (diameter = 0.06 μm). Also particle counters are not specific to soot in that they cannot discriminate between carbon particles and other kinds of particles.

3.2 DIRECT TRANSMISSION

Direct transmission, which is a measurement of light extinction by the soot particles, is simple to instrument and directly related to the mass concentration of soot. As will be shown, direct transmission does not have sufficient sensitivity, but discussion of this technique provides a basis for further treatment of more promising soot measurement techniques.

The light power (watts) transmitted through a cell of soot-laden gas is given by Beer's Law,

$$I = I_0 \exp(-A_E \rho L) \tag{3.2-1}$$

where I_0 is the original light power (watts), A_E is the specific extinction coefficient (m^2/g), ρ is the soot concentration (g/m^3), and L is the optical path length through the cell.

Solving for the soot density one has

$$\rho = \frac{1}{A_E L} \ln(I_0/I) \quad . \tag{3.2-2}$$

To determine the value of soot density to 10% accuracy, assuming the transmission measurement is made to 1% accuracy, the transmission (I/I_0) must be at most 90% (10% extinction). Transmission measurements of greater than 1% accuracy are difficult to make because of contamination of window surfaces, and detector instabilities.

The minimum sensitivity of direct transmission can now be determined assuming 90% transmission, 1 meter pathlength (maximum for an instrument usably sized), and a specific extinction of 10 m^2/g (see Roessler and Faxvog[10]).

$$\rho = \frac{1}{(10\ m^2/g)(1\ m)} \ln\left(\frac{1}{0.9}\right) = 11\ mg/m^3 \tag{3.2-3}$$

This minimum value is compared to the desired minimum sensitivity of 1 mg/m^3. The sensitivity of direct transmission for longer wavelengths is worse. Using the value of $A_E = 0.9\ mg/m^3$ at 10.6 μm from Ref. 10, one obtains a minimum detectable concentration of soot of 120 mg/m^3.

Other gas species may absorb light and interfere with the measurement of soot. For visible light, the major interference from jet engine exhausts is due to NO_2, which can be present at concentrations of 25 ppm at full power. For 25 ppm of NO_2 at STP, the extinction from NO_2, using the extinction coefficient measured by Hall and Blacet[11] of $A_E = 0.22\ m^2/g$ at 500 nm, is equivalent to 1 mg/m^3 of soot. This interference can be reduced somewhat to 0.4 mg/m^3 soot equivalent by operating at 600 nm, where extinction due to NO_2 is less ($A_E = 0.09\ m^2/g$ from Ref. 12). At infrared wavelengths, interferences from CO_2 and H_2O will be strong. Interferences due to absorbing gases can be overcome by using a reference cell method[6] where the soot particulates are filtered out and the background extinction due to interfering gases is measured. However, this correction is difficult to make in a real time device.

3.3 MODULATED TRANSMISSION

3.3.1 General Description

Direct transmission measurements of soot absorption have advantages of simplicity and a close relationship to the desired quantity – soot loading in mass per unit volume. However, soot levels of 1 mg/m^3 attenuate light at about 1% per meter, which is very difficult to measure with direct transmission because of window contamination and detector instabilities. Modulated transmission is a variation on the direct transmission technique that retains its advantages, but holds promise of allowing accurate measurements at attenuations of 1% per meter or less. This additional capability is attained by performing a rough equivalent of a reference "zero-absorption" measurement many times a second, by varying the sample density with an acoustic field.

A typical modulated transmission configuration is shown in Figure 3.3-1. A light source such as an incandescent bulb, filtered to the desired color bandwidth, is focused through a gas cell where the soot sample is subjected to a moderately intense acoustic wave. The cell is closed at one end and driven at a resonant frequency in a higher order mode by a loudspeaker at the other end. The light beam traverses a region of maximum gas density fluctuation, whereas the soot sample is admitted and exhausted by ports near regions of minimum fluctuation density, minimizing perturbation of sample lines by the acoustic field in the cell. The

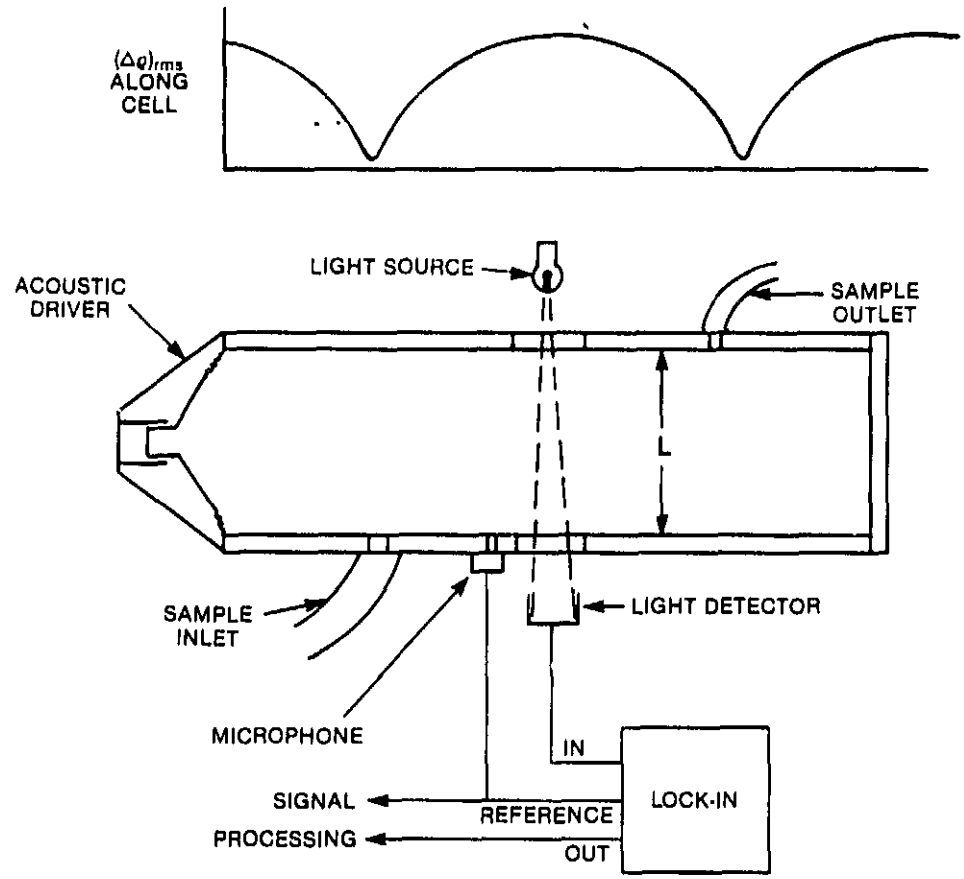

Figure 3.3-1. System configuration for modulated transmission measurement of soot concentration

transmitted light beam is detected by a vacuum photodiode. The small amplitude variation in the photodiode signal resulting from the acoustic modulation of the soot absorber density can be determined quantitatively from the output of a lock-in amplifier that uses the loudspeaker drive or a pressure transducer signal as a reference signal. The analysis of this system, developed below, shows that soot mass concentration can be determined from the rms variation and the average value of the photodetector signal, a measure of the rms acoustic pressure fluctuation, and the specific extinction coefficient of soot. A combined calibration constant of the detectors can be determined by filling the cell with a known concentration of absorber gas (such as NO_2).

3.3.2 Theoretical Principles

The transmitted light power (watts) through an absorbing medium in a cell such as that shown in Figure 3.3-1 is given by Beer's law:

$$I = I_0 \, T_w exp(-A_E \rho L) \tag{3.3-1}$$

I_0 is the original light power, T_w is the transmission of the optical elements (i.e., windows), A_E is the specific extinction coefficient (sum of the absorption and scattering coefficients expressed in m^2/g), ρ is the mass concentration of the soot in the gas, and L is the pathlength of the light through the cell.

In a practical sense, Beer's Law is valid for monochromatic radiation over negligible to moderate optical depth (typically, $0 \leqslant A_E \rho L \leqslant 3$). The upper limit on optical depth arises because of multiple scattering, which can return part of the light originally diverted from the beam by scattering. When broadband radiation is involved, Beer's Law must be integrated over wavelength, taking into account the variation of A_E with wavelength. However, in our case $A_E \rho L$ is expected to be small (< 1) at all probed wavelengths, so that the first two terms of the Taylor series expansion of $exp(-A_E \rho L)$ are sufficient. In this case the value of A_E given by,

$$\bar{A}_E = \frac{\int I_0(\lambda) A_E(\lambda) d\lambda}{\int I_0(\lambda) d\lambda} \tag{3.3-2}$$

can be used with Beer's Law with negligible error. Here $A_E(\lambda)$ and $I_0(\lambda)$ are the values of the specific extinction and the source intensity as a function of wavelength.

In modulated transmission the density in the cell is modulated. The transmitted light power is given by,

$$I + I'(t) = I_0 \, [T_w + T'_w(t)] \exp [- (\rho + \rho'(t)) \, A_E L] \; . \tag{3.3-3}$$

Here I is the value of the transmitted light averaged over a measurement period (typically one second for this application) while $I'(t)$ is the fluctuation. The factors T_w and $T'_w(t)$ account for the average and fluctuation of transmission through optical elements, and ρ and $\rho'(t)$ are the average and fluctuating values of the soot mass concentration. In this application the desired measured quantity is the averaged soot mass concentration, ρ, or the extinction per unit length, ρA_E. As noted above, we are primarily concerned with measurement of weak absorption values (e.g., 1% extinction or less, across a 10 cm path) and consequently, it is accurate to expand the fluctuation of the exponential function in Eq. (3.3-3) into its first two terms, i.e.,

$$I + I'(t) = I_0[T_w + T_w'(t)]\ [1 - \rho A_E L\ (1 + \rho'(t)/\rho)] \quad . \tag{3.3-4}$$

For adiabatic, isentropic, expansion/compression cycles, the gas density fluctuations are given by (assuming $\rho_g' < \rho_g$),

$$\rho_g'(t)/\rho_g = p'(t)/(\gamma p) \tag{3.3-5}$$

where $\rho_g'(t)$ and ρ_g are the average and fluctuating values of the gas density and p and $p'(t)$ are the average and fluctuating values of gas pressure, while γ is the ratio of specific heats ($\gamma = 1.4$ for N_2).

Calculations of particle motion in turbulent gas flows (Melling and Whitelaw[13]) that have been checked experimentally (Mazumder and Kirsch[14]) indicate that 1.3 μm diameter TiO_2 particles will follow the velocity fluctuations up to 1 kHz with 99% fidelity. Soot particles have a density of less than half that of TiO_2 and will have a greater frequency response. Thus soot particles in the size of interest (0.01 - 1.0 μm) will follow the gas pressure fluctuations up to 1 kHz and the soot density fluctuations, $\rho'(t)/\rho$, are given by the right hand side of Eq. 3.3-5. Substituting into Eq. 3.3-4 we have,

$$I + I'(t) = I_0\ [T_w + T'_w(t)][1 - \rho A_E L\ (1 + p'(t)/(\gamma p))] \quad . \tag{3.3-6}$$

A likely measurement procedure based on Eq. (3.3-6) would involve determination of the root-mean-square (rms) fluctuation of $I'(t)$ in a narrow frequency band around the acoustic frequency — a standard operation performed by a lock-in amplifier. Therefore, we separate the signal into its mean and time varying components. The mean signal is given by

$$I = I_0\ T_w(1 - A_E \rho L) \tag{3.3-7}$$

and represents the direct transmission measurement in the small extinction limit. The time varying signal is given by,

$$I'(t) = -\ I_0\ T_w\ [\rho A_E L\ p'(t)/(\gamma p)\ -\ (T'_w(t)/T_w) \tag{3.3-8}$$

$$+\ (T'_w(t)/T_w)\ \rho A_E L\ +\ (T'_w(t)/T_w)\ \rho A_E L\ p'(t)/(\gamma p)]$$

which is the modulated transmission measurement. We assume, subject to later discussion, that $T'_w(t)$ has no significant frequency components above, say 100 Hz, whereas the primary variation of $p'(t)$ is in a narrow, much higher frequency band (typically near 750 Hz). Furthermore, we ignore the last term, since it contains the product of two small quantities. Then only the first term in Eq. (3.3-8) will contribute significantly to the acoustic bandwidth rms average.

In that case, we have, taking the rms average of 3.3-8,

$$I_{rms} = I_0\, T_w \rho\, A_E L p_{rms}/(\gamma p) \quad . \tag{3.3-9}$$

Now the mass fraction of soot can be determined for the modulating transmission measurement,

$$\rho = \left[\frac{\gamma}{T_w L A_E}\right]\ \left[\frac{I_{rms}}{I_0}\right]\ \left[\frac{p}{p_{rms}}\right] \quad . \tag{3.3-10}$$

In practical direct transmission measurements, the cell is first filled with a nonabsorbing gas and the transmitted light power is measured (Equation 3.3-1),

$$I_N = I_o T_w \quad . \tag{3.3-11}$$

Now the transmitted power, I, is measured with the soot present and the density is given by,

$$\rho = \frac{1}{A_E L} \ln\left[\frac{I_N}{I}\right] \quad . \tag{3.3-12}$$

The difficulty in direct transmission measurements can be seen when in the limit of small extinction this is approximated as,

$$\rho \doteq \frac{1}{A_E L} \left[\frac{I_N - I}{I}\right] \quad . \tag{3.3-13}$$

In the direct transmission measurement, the soot density depends on the difference of two quantities which are different by only a few per cent. The modulated transmission measurement, Eq. (3.3-10), depends on the magnitude of individual quantities, which is the primary advantage of the technique.

3.3.3 Modulated Transmission Proof of Principle Experiment

Since the modulated transmission technique was highly rated and, insofar as we know, has not been tested to date, a preliminary experimental test was performed to demonstrate the principle and search for potential problems. Modulated transmission was used to measure small amounts of NO_2 (200 ppm in N_2), which simulated soot as the attenuation species. As seen in Table 3.3-1, this level of NO_2 has the same light attenuation as 25 mg/m^3 of soot, which is a typical soot concentration of older jet engines. Since the concentration of the NO_2 gas was known, the NO_2 extinction coefficient was measured by modulated transmission and by direct transmission, and compared to literature values. In practical application, an extinction coefficient is determined from calibration measurements or literature values and the density of the soot is measured.

An aluminum tube (100 mm i.d. by 460 mm long) was used as the absorption chamber. The chamber was closed at one end and driven by a loudspeaker through a thin Teflon membrane used to seal the cell at the open end. Speaker power was drawn from a 15 watt audio amplifier excited by a signal generator.

Table 3.3-1

Comparison of extinction coefficients of NO_2 (200 ppm) and soot (25 mg/m^3) at 1 atm pressure. Extinction coefficient for NO_2 from Hall et al.,[11] and for soot from Roessler and Faxvog[10].

	ρ (g/m^3)	A_E (m^2/g)	ρA_E (m^{-1})	λ (nm)
NO_2	0.38	0.65	0.25	420-480
Soot Specification	0.025	10	0.25	514.5

Pressure fields inside the cylinder were mapped at twelve tapped ports along the length of the chamber using a 5 mm dia. microphone and amplifiers calibrated by a pistonphone. Root-mean-square pressure fluctuations up to approximately one millibar (accuracy in these rough measurements is estimated to be within a factor of 2) were obtained using several watts drive power, at the first three resonant frequencies of the chamber (167, 420, and 750 Hz). A theoretical analysis of the acoustic fields and resonance frequencies showed excellent agreement with the experiments. The pressure waves were close to sinusoidal up to a drive power of about 8 watts, where pressure wave distortions could easily be seen on an oscilloscope, and could also be heard.

A microscope illuminator lamp connected to a stable dc power supply provided the probe beam of light. This beam was filtered to contain only the 420-480 nm band, so that the average extinction coefficient would be determined over a defined bandwidth. The light beam traversed the cell along a diameter (100 mm) passing through glass windows attached with epoxy cement. The light was detected by a vacuum photodiode across a 1 MΩ load resistor (and capacitance < 100 pF). The resulting voltage signal was filtered to a narrow passband (≈ 100 Hz) around the sound frequency and displayed on an oscilloscope. A lock-in amplifier measured the detector signal, using the pressure signal as the phase reference.

A premixed mixture of two hundred parts per million of nitrogen dioxide in nitrogen served as the absorption standard and was passed through the cell at room pressure. Modulated transmission measurements were undertaken at the third resonance (750 Hz) because the pressure fluctuation field at this frequency has a maximum very near the center of the tube, where the windows were located, and a node on either side of the window, where inlet and outlet ports could be located without encountering a high acoustic field.

In the modulated absorption experiments, p_{rms}/p was set equal to 1×10^{-3} (0.1%) as measured by the calibrated microphone, by adjusting the loudspeaker drive. The resulting measurements of I_{rms} and $T_w I_0$ gave detector signals of 1.7×10^{-4} volts and 9.75 volts, respectively. Substituting these values into Eq. (3.3-10), where ρ_a is the density of NO_2 in cell (200 ppm), we obtained an extinction coefficient of $A_E = 0.62$ m^2/g.

Direct transmission through the absorbing gas mixture in the cell was also measured by alternately filling the cell with this mixture and with pure nitrogen gas. The specific extinction coefficient is given by Eq. (3.3-12)

$$A_E = \frac{1}{\rho_a L} \ln\left[\frac{I_N}{I}\right] \quad . \tag{3.3-14}$$

Five direct transmission measurements had an average of 97.9% transmission (I/I_N) across the 100 mm optical path through the cell with a standard deviation of 0.4%. This gives a value of $A_E = 0.56 \pm 0.1$ m^2/g. The relatively large standard deviation and long time (15 minutes) required for these measurements illustrate the difficulties associated with direct transmission measurements of low absorption.

The measurements of A_E from direct transmission and modulated transmission are shown in Table 3.3-2 along with a literature value[11] that has been averaged for the wavelength range of the light source (420-480 mm). The moderate difference between the direct and modulated values in Table 3.3-2 is within the experimental standard deviation for the former, but could also arise from errors in the rms pressure measurements obtained using the microphone, since no special efforts were made in these initial tests to validate the absolute calibration of this microphone. In practice, as noted previously, measured attenuation by NO_2 (preferably at somewhat higher concentration) could be used to calibrate the modulated

Table 3.3-2

Average extinction coefficients (420-480 nm) for NO_2 determined from measurements of 200 ppm of NO_2 and literature studies.[11]

Technique	A_E (m^2/g)
Direct Transmission	0.56
Modulated Transmission	0.62
Literature Value	0.65

transmission cell (in effect, calibrating the microphone). This calibration procedure can be based simply on comparison of direct and modulated transmission measurements. The calculated transmission value is in satisfactory agreement with the measurements, given the expected error in this value, since no attempt was made to weight the absorption vs. wavelength by source, detector, and filter spectral characteristics.

The blue light attenuation of 200 ppm NO_2 in air is close to 25% per meter, high enough to measure accurately (with some difficulty). Thus the successful measurements summarized in Table 3.3-2 do not in themselves demonstrate capability to measure the weaker absorption values of interest in the present application (1% per meter). However, we were able to follow the modulated absorption signals with good signal-to-noise down to less than 10% of the full value as pure N_2 slowly mixed into the cell, lending support to our expectation that this approach will be useful for transmission values as small as 1% per meter. Construction of an improved cell, in order to minimize background signals from window vibration, should improve the lower detectibility limit. Window vibrations cause fluctuations of the window transmission at the driver frequency, making the T_w' terms in Eq. (3.3-8) important at low soot concentration levels.

3.3.4 Potential Problems

The most serious potential problem of a soot concept based on soot particle light extinction is the determination of the extinction coefficient. As reported by Roessler and Faxvog,[10] the extinction coefficient for soot at visible wavelengths will vary 20% depending on the combustion device. These variations are traced to the extinction coefficient's dependence on particle size distribution, particle shape, and organic fraction, which all depend on the specific combustion process. Modulation transmission's direct measurement of light extinction, ρA_E, can also be seen as a potential advantage since many unfavorable aspects of soot emission are due to its visibility, which is related to its extinction coefficient.

Modulated transmission measurements also depend on accurate determination of the rms pressure modulation. We have found that adequate values can be obtained from calibrated microphones for conditions near ambient. However, determination of rms pressure values at the high pressure and temperature specified in the Appendix may be more difficult. Also, construction of a cell driver that will withstand elevated temperature and pressure is a problem.

Other potential problems related to modulated transmission are the effect of fluid flow on the pressure field at the high flow rates necessary to obtain the required frequency response

(1 per sec), and vibration of the cell, which may restrict the lower detectibility limit. In addition, the presence of interfering gases that attenuate the light could give erroneous results at lower soot concentrations. The major interferent in jet engine exhausts at visible wavelengths will be NO_2. For 25 ppm of NO_2 at STP, typical of full load conditions, the attenuation will be equivalent to 1 mg/m^3 at 500 nm and 0.4 mg/m^3 at 600 nm. At infrared wavelengths, interference from H_2O and CO_2 is a problem. These interferences can be eliminated by use of a reference cell[6] but real-time measurement with an additional cell is difficult.

3.3.5 Summary

1. Error sources, expected accuracy, response time, and concentration range.

   The expected accuracy of the technique is ± 20% based on the uncertainty in the soot extinction coefficient due to the effects of particle size distribution, particle shape, and composition (i.e., organic fractions). The response time and the lower limit of the concentration range are yet to be determined and require further study.

2. Principal components

   The recommended system would consist of the following components:

   - Absorption cell with driver, windows
   - Light source, detector, filters, lenses
   - Lock-in amplifier
   - Microphone or rms pressure sensor
   - Signal, analysis, and display equipment.

3. Calibration

   A cell would be filled with a known concentration of NO_2 gas and the NO_2 specific extinction coefficient for the wavelength range of the source and detector would be determined by direct transmission. Next the detectors would be calibrated by making a modulated transmission measurement on the same NO_2 mixture. The soot specific extinction coefficient would be determined from literature values or by measurement using modulated transmission in combination with a gravimetric measurement.

4. Significant disadvantages

   The measurement is based on the light extinction of soot that can be variable depending on the soot particle distribution, shape (index of refraction), and organic fraction. Other gases, such as NO_2, can interfere with the measurement.

5. Key questions for further study

   The modulated transmission cell needs to be redesigned to improve detectibility limits (lower wall vibration) and allow high-temperature and high-pressure operation (improved driver and more rugged microphone). The effect of the high flow rates (needed for fast response) on the pressure field needs to be investigated. Also the importance of interfering gases such as NO_2 needs to be determined.

3.4 CROSSED BEAM ABSORPTION COUNTER (CBAC)

3.4.1 General Description

The Crossed Beam Absorption Counter (CBAC) concept is one of a class of particle measurement approaches called particle counters that function by measuring one particle at a time. They are distinguished by an active volume small enough so that there is a negligible probability of having more than one observable particle in the active volume. When based on scattering (see Section 3.1.2), these approaches can provide particle size distribution information down to about 0.04 μm diameter, under favorable conditions. The CBAC is based on light extinction rather than scattering with the advantage of being able to preferentially measure soot. The light extinction is measured as one particle passes through a set of interference fringes formed by the crossing of two laser beams.

3.4.2 Theoretical Principles

A representative CBAC configuration is shown in Figure 3.4-1. Two beams derived from the same laser cross at the measurement volume at an angle of 90°. The beams are each given a square cross section with a constant intensity (within 10%) across the beam. As we will see, this is needed to measure the particle mass to 10% accuracy. The square cross section is obtained by expanding the beams, passing them through a square aperture, and imaging the aperture into the measurement volume. The power of the beams after passing through the aperture can be determined as follows. The power at a radius r_0 of the Gaussian beam is given by:

$$I_r(r_0) = I_c\, e^{-(r_0/r_e)^2} \tag{3.4-1}$$

where r_e is the radius at the 1/e points and I_c is the intensity in the center of the beam. Integrating this expression, the total power contained in a Gaussian beam that is passed through a circular aperture r_a is,

$$I_t(r_a) = I_0\,[1 - e^{-(r_a/r_e)^2}] \tag{3.4-2}$$

or

$$I_t(r_a) = I_0[1 - I_r(r_a)/I_c] \tag{3.4-3}$$

where I_0 is the total beam power unattenuated,

$$I_0 = \pi r_e^2\, I_c \quad . \tag{3.4-4}$$

Thus, a beam which is passed through a circular aperture where the intensity of the outer edge is at least 90% of the center ($I_r(r_0) = 0.9\ I_c$) has a radius

$$r_a = 0.325 r_e \tag{3.4-5}$$

and a total power

$$I_t(0.325 r_e) = 0.1\ I_0 \tag{3.4-6}$$

Only 10% of the power will remain after passing through the aperture. Here we will choose a square aperture with the equivalent area of a circular aperture. The length of the side of the square is

$$d_s = 0.325 \sqrt{\pi}\ r_e$$

or

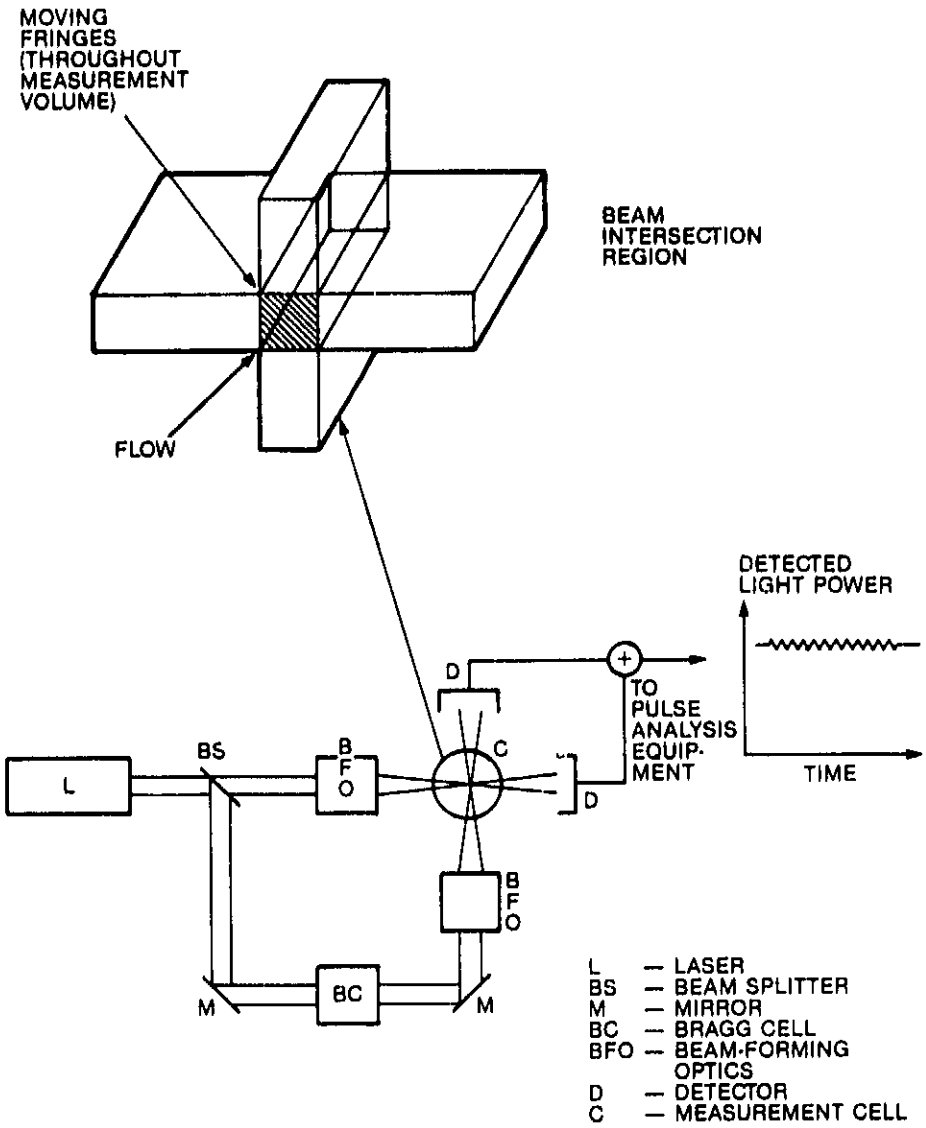

Figure 3.4-1. Experimental configuration for crossed beam absorption counter (CBAC) showing beam intersection region in detail

$$d_s = 0.575 r_e \tag{3.4-7}$$

The lowest intensity will be 85% of the center at the corners of the square ($r_0 = 0.406 r_e$). This will still be well within the ±10% average intensity needed for the measurement.

At the crossing point shown in Figure 3.4-1, interference between the beams sets up a striped interference pattern. It is advantageous to cause the strips to move by frequency–shifting one of the beams, using a Bragg cell, for example. The configuration shown in Figure 3.4-1 closely resembles that used in real fringe laser velocimeters; the fringe spacing is given by,

$$d_f = \frac{\lambda}{2 \sin(\alpha/2)} \tag{3.4-8}$$

where α is the beam crossing angle. In the present case, the transmitted power in both beams is monitored, rather than the scattered light. A small (compared to stripe width) absorbing particle traveling through the striped pattern will diminish the transmitted power only when it intercepts a bright stripe. Thus the total transmitted beam power will display a time variation of the form

$$I = I_0 \left[1 - a_e \left(1 - \sin 2\pi f_d t\right)\right] \tag{3.4-9}$$

during the time a particle is in the beam intersection volume, where I_0 is the total power in both beams and f_d is the frequency of the intensity modulation of the beams given by,

$$f_d = u_p / d_f + f_0 \tag{3.4-10}$$

Here f_0 is the Bragg cell frequency, and u_p is the particle velocity component normal to the fringe pattern. The time-averaged particle extinction, a_e, is given by

$$a_e = \sigma_e / a_0 \tag{3.4-11}$$

where a_0 is the area of each beam normal to the direction of propagation. For soot particles with radii smaller than about 0.1 μm (Rayleigh regime), the extinction cross section σ_e is proportional to particle volume, and given by

$$\sigma_e = \frac{4\pi}{3} r^3 \rho_c A_E \tag{3.4-12}$$

where ρ_c is carbon density ($\rho_c \simeq 2.0$ grams/cm^3), r is particle radius and A_E is the specific extinction coefficient of soot. Using a selected value for A_E

$$A_E = 8 \times 10^4 \text{cm}^2/\text{g}$$

we obtain

$$\sigma_e = (6.7 \times 10^5 \text{cm}^{-1}) r^3 \tag{3.4-13}$$

Thus the sinusoidally varying part of the signal has (peak-to-peak) amplitude

$$I_{p-p} = 2 a_e I_0 = (1.3 \times 10^6 \text{cm}^{-1}) \frac{I_0}{a_0} r^3 \tag{3.4-14}$$

with resulting root-mean square amplitude

$$I_{rms} = \frac{a_e I_0}{\sqrt{2}} = (4.7 \times 10^5 \text{cm}^{-1}) \frac{I_0}{a_0} r^3 \tag{3.4-15}$$

This signal will persist for a particle transit time of $t_0 = d_0 / u_p$, where d_0 is the width of the crossing point of the two beams.

In a well-designed system, the limiting noise over which this signal must be detected will be signal shot noise, whose mean square equivalent amplitude is

$$(I_N)_{rms} = \left[\frac{2 I_0 h\nu B_0}{q}\right]^{1/2} \tag{3.4-16}$$

assuming weak absorption ($\sigma_e << a_0$) so that the detected power is nearly I_0. Here q is the detector quantum efficiency, $h\nu$ is the energy per photo . ($\approx 4 \times 10^{-19}$ joule for blue-green light) and B_0 is the observed signal-bandwidth, which is optimally determined by the persistence of a signal from a single particle; i.e.,

$$B_0 \simeq t_0^{-1} \tag{3.4-17}$$

Thus the signal SNR for detection of a single particle is

$$SNR = \frac{I_{rms}}{(I_N)_{rms}} = (3.3 \times 10^5 cm^{-1}) \frac{r^3}{a_0} \left[\frac{q I_0 t_0}{h\nu}\right]^{1/2} \tag{3.4-18}$$

A minimum detectable particle size r_{min} is given by setting SNR = 1;

$$r_{min}^3 = (0.30 \times 10^{-5}\text{cm}) a_0 \left[\frac{h\nu}{q I_0 t_0}\right]^{1/2} \tag{3.4-19}$$

However, the product $I_0 t_0 / a_0$ is likely to be limited to 0.1 J/cm^2, to avoid vaporizing the carbon particles (see LIN Section). Thus we find

$$r_{min}^3 = (0.94 \times 10^{-5}\text{cm}^2/\text{J}^{1/2}) \left[\frac{h\nu a_0}{q}\right]^{1/2} \tag{3.4-20}$$

It is probable that beams can be focused into 10 μm cross sections with suitably sharp edges by expanding the beams, passing them through a square aperture, and focusing the aperture image into the measurement volume using low power microscope objectives with a focal length of about 1 cm. This configuration should also minimize the effect of beam wander due to index of refraction fluctuations. The beam area is 10^{-10} m^2 and, from Eq. (3.4-20) (assuming q = 10%), the minimum observable particle radius is

$$r_{min} = 0.027\ \mu m. \tag{3.4-21a}$$

$$d_{min} = 0.054\ \mu m. \tag{3.4-21b}$$

The minimum diameter for CBAC (0.05 μm dia.) is remarkably close to the limit for scattering (0.06 μm dia.) even though the phenomena are different.

The concentration range of the instrument can be determined as follows. For a crossing angle of 90°, the active volume is 10^{-15}m^3, allowing a maximum observation number density, N_{max}, of 10^{14} per cubic meter to satisfy the one-particle-at-a-time criteria. Assuming a soot density, ρ_c, of 2 g/cm^3, and an average soot diameter, d_{ave}, of 0.1 μm, the maximum soot concentration is,

$$\rho_{max} = \rho_c \left(\frac{\pi d_{ave}^3}{6}\right) N_{max} = 100\ \text{mg/m}^3 \quad . \tag{3.4-22}$$

The lower limit of the mass concentration range is determined by the particle counting rate. One hundred particle diameters are needed to determine the mass average diameter of a monodisperse distribution to 10% accuracy, as the particle arrival times follow Poisson statistics. Thus a particle counting rate, R, of 100 per second is required for a one second time response. The particle number density is given by,

$$n = \frac{R}{a_o u_p} \quad . \tag{3.4-23}$$

For a beam area of 10^{-10} m^2 and a particle velocity of 1 m/s, the minimum number density is 10^{12} per cubic meter, which is equivalent to 1 mg/m^3. Thus the concentration range of the instrument is 1-100 mg/m^3 for narrow soot particle distributions of 0.1 μm mass average diameter.

The corresponding soot concentration range versus mass-weighted average particle size is shown in Figure 3.4-2. The dashed region indicates the diameter and soot concentration ranges of interest from 0.03-1.0 μm diameter and 1 to 100 mg/m^3. To the left of line AB, soot particles are too small to be observed. Above BC, particle number densities are too great for single particle counting, while below AD the data rate is too low. Two shortcomings of the CBAC instrument can be seen. It cannot measure the smallest particles of potential importance (below 0.05 μm diameter). Also, as indicated by the boundary AD, the instrument has difficulties measuring soot concentrations at large soot diameters because of its slow time response or high data rate requirements. The instrument must measure a large enough sample of particle diameters to obtain a statistically accurate mass average. Here, we have only considered the random arrival rate of the particles in determining this boundary which is

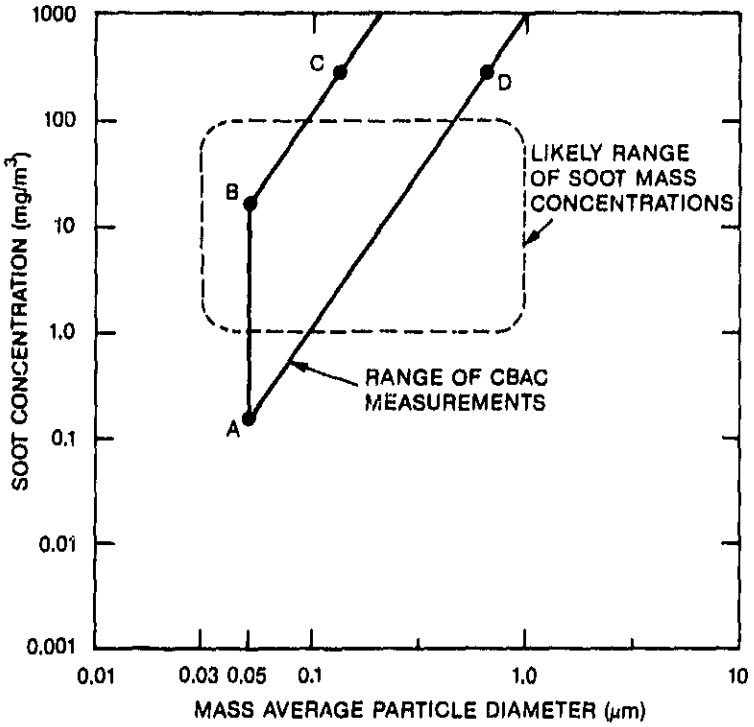

Figure 3.4-2. Comparison of CBAC measurement range and the likely range of soot concentration versus particle size

accurate for narrow distributions of particle size. Broad distributions of particles require a larger number of particles to determine an accurate mass average and less of the region of interest in Figure 3.4-2 can be measured in a one second time response.

The laser power requirements for an energy exposure of 0.1 J/cm^2 can be satisfied by an initial laser power of 80 mW at the assumed particle velocity of 1 m/sec, yielding a particle exposure time, $t_0 = 10\ \mu s$. Here we have taken into account the 90% attenuation of the square apertures that provide the square cross sections. The fringe spacing (see Eq. (3.4-8)) is 0.35 μm, which will give about 30 fringes in the measurement volume. The signal frequency will be 2.8 MHz, which is a convenient operating frequency for the assumed operating conditions, and an additional frequency shift (i.e., Bragg cell) would not be needed.

3.4.3 Potential Problems

Considerable alignment effort is required to accurately cross two beams of such a small diameter. Furthermore, we have not addressed the practical equipment requirements. The detectors and subsequent electronics will have to view a signal with modulation amplitude as small as 10^{-7} of the average value. Special care will be needed to avoid mixing of the beams through stray light scattering, which could produce heterodyne signals comparable to the absorption signal. For particle diameter bigger than about 0.1 μm, scattering becomes significant, and soot particles will no longer be sensed preferentially (see Roessler and Faxvog[15]). The instrument has an inherently slow time response for large particles because it requires a large number of particles to obtain an accurate mass average. Considerable data analysis will be required to draw reliable conclusions about particle distribution, which may have significant components out of the range shown in Figure 3.4-2. Thus, although the CBAC concept shows some promise, its problems appear too serious to allow development to a robust test instrument within a few years.

3.4.4 Summary

1. Error sources, expected accuracy, response time, and concentration range.

Soot concentration is determined from CBAC data by summing the mass contribution of particles in each size range, and dividing by the total sampled volume,

$$V_s = a_0 u_p t_0$$

where u_p is the gas flow velocity in the measurement region, a_0 is the area of this region perpendicular to the flow direction, and t_0 is the measurement duration. The following errors can be significant in this determination:

a. Unmeasured small particles: The magnitude of this error depends on particle size distribution. Most distribution measurements show mass concentrated primarily in particles larger than 0.03 μm radius, except in early formation regions in combustion zones. Estimated error in the soot concentration is less than 10% relative standard deviation.

b. Particle shape effects: The extinction cross section for a given particle mass depends somewhat on its shape. Our estimate of the error introduced by this effect, for visible light illumination, is 10%. A larger error is expected in the infrared because of enhanced shape effects at longer wavelengths.

c. Uncertainty of specific absorption and/or variation with soot composition: 10%

d. Corrections for large particles ($r > 0.1\ \mu$m): 10%

e. Sampling volume error: 10%

f. Alignment error. If alignment is checked frequently (by maximizing detection rate): 10%

If the estimated error sources are assumed independent, then their combined effect (square root of sum of squares) yields an expected error of 30% relative standard deviation.

Adequate time response is expected from the CBAC technique under nearly all soot conditions except for low concentrations of large particles. Furthermore, it should be able to handle the full range from 1.0 to 100 mg/m^3 with the exception of high concentrations of very small particles. Range and time capability are illustrated in Figure 3.4-2.

2. Principal components

- One watt argon laser
- Vacuum photodiode detectors (2)
- Mirrors, beam splitters, stop to form square beams and microscope objectives
- Test cell
- Burst analyzer
- Computer

All of these components are commercially available with expected adequate performance, with the exception of the test cell, which appears to present no serious design difficulties, and the burst analyzer, which can be a filter at the signal frequency (~ 3 MHz) followed by an RF detector and a pulse height analyzer. Burst frequency and duration information are also useful, allowing direct calculation of sampled volume, and a valuable data quality check. Some standard laser velocimetry burst counters may be appropriate for this purpose, provided they have burst amplitude signals with wide dynamic range (at least 100:1). The computer reads out the pulse height distribution after each measurement period, multiplies each size group by its equivalent volume, applies any necessary corrections, such as for large particles, checks for some errors (wrong laser power, bursts near limits of dynamic range, too high data rate, overly short or long bursts indicating poor alignment) and outputs data in a clear format.

3. Calibration

The major requirement for accurate calibration of this system is proper alignment. Positive alignment can be accomplished by viewing an adjustable target, oriented to intercept the beam intersection through a microscope mounted on the chamber. Viewing should be through a TV camera and monitor for laser safety. When the beams appear aligned and focused on the monitor, final adjustments are obtained by maximizing the signal from a stable soot source. Subsequently individual particle volumes can be obtained directly from the ratio of a modulated signal to its average value, and from knowledge of the interaction volume dimensions which are fixed geometrically. Likewise, overall concentration can be obtained from the particle count rates and active volume dimensions. Thus, once the system is properly aligned, calibration is obtained from known or easily measured quantities. However, considerable operator skill will be required for alignment to the required precision, on the order of several tenths of a milliradian, for the beam dimensions assumed above. Furthermore, stability of this alignment may be shortlived in the presence of vibration and temperature fluctuations.

4. Significant disadvantages

   a. Cannot measure particles with diameters smaller than about 0.05 μm.

   b. Requires expensive laser, TV alignment system (for eye safety) and LV burst counter. Total system cost probably greater than $40,000.

   c. Establishment and frequent verification of required precise alignment will require considerable operator skill.

3.5 TAPERED ELEMENT OSCILLATION MICROBALANCE (TEOM)

3.5.1 General Concept Description

One of the positive responses from the vendor survey was a Tapered Element Oscillating Microbalance (TEOM) instrument. The instrument filters the soot-laden gas and measures directly the desired quantity—mass concentration of soot in the gas. The technique alleviates the major disadvantage of filtering techniques: their long time response. The instrument collects the soot in a filter element mounted on the end of a hollow vibrating tube, where the vibration frequency gives a real time measure of the collected particulate mass. The technique still has a major disadvantage of filtering techniques—sensitivity to total particulate mass including organics, noncarbonous inorganics, water, and volatiles. Some of these interferences can be overcome by sample conditioning.

Operation of the TEOM is shown in a simplified manner in Figure 3.5-1. The TEOM instrument consists of a vertically mounted tapered hollow tube, fixed at the wide end on the bottom with a changeable filter element at the narrow end on the top. An exhaust sample is drawn through the filter element down the hollow TEOM tube. The tapered tube is maintained in continuous oscillation with the frequency of oscillation being accurately monitored. As particulate deposits on the filter element, the frequency of oscillation changes in relation to the mass added. The tapered element is located in an oscillating electric field, maintained between two field plates, which causes the element to oscillate in the light path of a light emitting-diode/phototransistor pair. The oscillating voltage output from the phototransistor is amplified and used as a feedback signal through a conductive path in the tapered element to interact with the electric field and maintain the oscillation. The oscillating voltage is also sent through a counter to the instrument microprocessor.

3.5.2 Theoretical Principles

The TEOM has been demonstrated to behave as a harmonic oscillator with the frequency, f, related to the effective mass, m_e, and a restoring force constant, K, by the following:

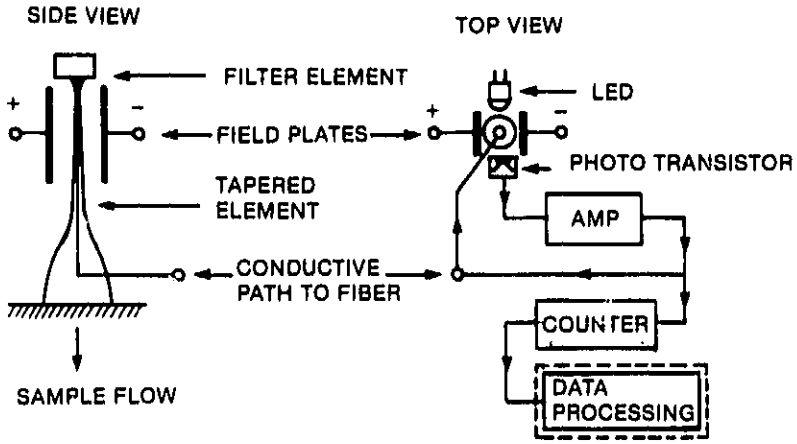

Figure 3.5-1. Schematic representation of tapered element oscillating microbalance (TEOM)

$$4\pi^2 f^2 = \frac{K}{m_e} \tag{3.5-1}$$

or

$$m_e = \frac{K_0}{f^2} \tag{3.5-2}$$

where

$$K_0 = \frac{K}{4\pi^2} \tag{3.5-3}$$

The effective mass, m_e, at any given time consists of the mass of the filter element, m_f, the effective mass of the tapered element, m_o, and the total mass particulate loading, m_p, which gives,

$$m_e = m_f + m_o + m_p \tag{3.5-4}$$

Changes in the effective mass, Δm_e, can only be due to changes in the particulate mass loading, Δm_p, which is given by,

$$\Delta m_p = K_o \left(\frac{1}{f_2^2} - \frac{1}{f_1^2} \right) \tag{3.5-5}$$

where the tube vibration frequency before and after the mass addition is f_1 and f_2, respectively.

Determination of K_0 is an instrument calibration performed by addition of a known mass, Δm_e, to the filter elements and measurement of the oscillation frequency before and after the mass addition. From Eq. (3.5-5), the effective force constant is,

$$K_O = \Delta m_e \left(\frac{1}{f_2^2} - \frac{1}{f_1^2} \right)^{-1} . \tag{3.5-6}$$

The TEOM instrument has been used to measure smoke from a variety of combustion sources including fluidized beds,[17] industrial power plants,[16,18] diesel engines,[19] and gas turbine engines.[20] Modifications of TEOM have been made to operate at high pressure[17] (700 kPa), and high temperature[21] (1240 K) which satisfy the smoke meter requirements of handling a gas at pressures and temperatures up to 350 kPa and 430 K.

The minimum mass concentration that can be measured at the required accuracy is given by,

$$\rho_{\min} = g(\phi,t)/\phi \tag{3.5-7}$$

where $g(\phi,t)$ is the mass sensitivity (g/sec) of the TEOM, ϕ is the filter flowrate (cc/sec), and t is the measurement time (sec). The mass sensitivity, $g(\phi,t)$, will be a function of the filter flowrate and the measurement time for a given hollow tube and filter element construction. For a flowrate of 50 cc/sec and a measurement time of 10 seconds, the mass sensitivity is 0.05 μg/sec[19] and the minimum density is (Eq. 3.5-7),

$$\rho_{min} = 1 \text{ mg/m}^3$$

Thus 10 seconds is required to measure the minimum concentration — rather than the one second specified in the General Smoke Meter Requirements (see Appendix). It is possible that a higher flowrate would produce a response time closer to one second. However, this possibiliy depends on the dependence of g on ϕ and t; that dependence has not been fully explored, particularly for condition found in proximity to jet engines.

3.5.3 Potential Problems

As a filtering technique, TEOM does not differentiate between carbonaceous matter and other particulates (inorganics, condensates) as all the particulate mass is collected. For example, the problem of condensation followed by evaporation has led to observations of negative particle mass loadings. [19,20] Errors may result from low filtering efficiency for the small particles, leakage around the filter element, flow of particles away from the element which deposit on the walls, variation of the spring constant with temperature, drag changes with pressure, and interference from external acoustic noise and external vibration.

Some of these problems can be solved by careful design and operation. Water condensation can be controlled by operation above 373 K. Corrections for pressure effects on drag and temperature effects on the spring constant can be made through calibration. The major shortcoming of the instrument is the frequency response. At low soot loadings (1 mg/m^3), the frequency response is limited by the sample flow rate through the filter element and the time to acquire a measurable mass. With the present instruments, about 10 seconds are required to make a measurement at low soot levels to the desired accuracy.

3.5.4 Summary

1. Error sources, expected accuracy, response time, and concentration range.

   Carbon loading measurement errors can result from calibration error, overly short measurement times, imperfect filtering, condensation and/or evaporation on the filter element, sensitivity to constituents other than carbon, leakage around the filter element, interactions between the flow and tapered element motion, and interference from external acoustic noise. Calibration effects are discussed subsequently. Field experience with this equipment indicates that accuracy with careful operation should approach ± 10 to 20%. Sample conditioning to prevent condensation (or operation above 373 K) and prevention of leaks around the filter element are important requisites for accurate operation. For higher temperatures, the spring constant variation as a function of temperature must be included in the calculation to provide accurate measurements. At low mass loadings, time response is limited by the mass resolution of the instrument and the mass flow rate through the filter. (At very high flow rates, turbulence will add noise to the tapered element oscillation, and filter efficiency will suffer.) With present instruments about 10 seconds appears to be required to measure loadings of 1 mg/m^3. On the other hand, linear response is retained as the filter collects up to 500 mg. Thus loadings of 100 mg/m^3 can be sampled for hours at a typical flow rate of 50 ml/sec, yielding convenient operation over the full expected range from 1 to 100 mg/m^3.

2. Principal components.

   a. Commercially available complete system, including sampling head, sampling pump, gas flow controls, calibration apparatus, and microprocessor-based analysis and display unit.

b. Appropriate sampling lines.

3. Calibration

   a. Introduction of known mass on tapered element.

   b. Weight determination of filter compared to indicated integrated mass load.

   c. Determination of filter efficiency by additional filtering, comparison with optical techniques, or resort to literature values.

4. Significant disadvantages

   a. Collection of total particulate mass including noncarbonaceous particles.

   b. Measurement time longer than 1 sec for light loadings.

5. Key questions for further study

   a. Investigate means of decreasing the sample time.

   b. Determine the magnitude of the interference from the expected acoustic and vibration conditions in the engine test cell.

3.6 LASER-INDUCED INCANDESCENCE (LIN)

3.6.1 General Description

Soot particles are detected in the laser-induced incandescence (LIN) technique by heating them to incandescent temperatures with a laser operating at one wavelength, and monitoring their incandescence at other, preferably shorter wavelengths. LIN has been identified as a primary undesirable background source in Raman measurements in sooting hydrocarbon flames.[22] The strength of that phenomenon becomes an advantage when it is desired to measure low-level concentrations of soot. Preliminary indications are that LIN is specific to soot absorption (in distinction to gas absorption). Estimates of the induced incandescence characteristics also indicate that LIN possesses sufficient sensitivity to measure concentrations much lower than 0.1 mg/m^3, and contains information regarding size distributions and volatile fractions. Furthermore, the LIN technique is insensitive to acoustic noise. However, closer examination reveals several potential problems that arise from the necessarily strong perturbation of particles as they are heated to incandescence. Outgassing of volatile adsorbates and surface chemical reactions are two of the resulting phenomena that may make LIN data difficult to interpret.

3.6.2 Theoretical Principles

Absorbing particles exposed to laser beams of moderate to high irradiance (near and above 10^4 watts/cm^2) are heated extremely rapidly until some cooling mechanism (e.g., vaporization or conduction) becomes important. The initial heating rate $d\theta/dt$ is given by

$$\frac{d\theta}{dt} = \frac{I_a \sigma_a}{C_c \rho_c (4\pi r^3/3)} = \frac{I_a A_A}{C_c} \tag{3.6-1}$$

Here θ is the particle temperature, C_c is the carbon heat capacity, ρ_c is carbon density, and I_a is incident beam power per unit area. The absorption cross section and the specific absorption coefficient are σ_a and A_A and r is the particle radius. Using the representative values, C_c = 2.1 J/gram °C and $A_A = 8 \times 10^{-4}$cm^2/g

$$\frac{d\theta}{dt} = 3.8 \times 10^4 \left(\frac{\text{cm}^2\ ^\circ\text{C}}{\text{J}}\right) I_a \left(\frac{\text{watts}}{\text{cm}^2}\right) \tag{3.6-2}$$

Thus, neglecting losses, an incident intensity of 10^6 watts/cm^2 in the visible will increase the particle temperature at a rate of 3.8 x 10^{10} °C/s, and will raise a pure carbon particle to its vaporization temperature (ca. 4500 K) in about 0.1 microseconds.

If the laser power is turned off when the particles approach the temperature where vaporization becomes significant, then straightforward calculations indicate that small particles will cool primarily by conduction. The initial cooling rate depends on particle size, such that for particles with radii $\leqslant 0.1\ \mu$m (i.e., smaller than the molecular mean free path at STP).

$$\frac{d\theta}{dt} = \frac{-3P\ C_g(\theta - \theta_o)}{C_c \rho_c r} \left[\frac{M}{2\pi N_A\ k\ \theta_o}\right]^{1/2} \tag{3.6-3}$$

where P, C_g, θ_o, and M are the surrounding gas pressure, specific heat, temperature, and molecular weight, while N_A and k are Avogadro's number and the Boltzmann constant. Using representative average values in consistent units

$$P = 1 \times 10^5 \text{ Pa (760 Torr)}$$

$$C_g = 1.2 \times 10^3 \text{ J/kg–K}$$

$$M = 29 \times 10^{-3} \text{ kg/mole}$$

we find

$$\frac{d\theta}{dt} = -4.9 \times 10^9 \text{ K/s} \tag{3.6-4}$$

for a 0.1 μm radius particle. Thus, in one microsecond the particle will lose most of its thermal energy.

Larger particles will cool at a substantially slower rate, not only because of the 1/r dependence in Eq. (3.6-3), but also because of the transition from molecular to continuum conduction cooling. This transistion begins at particle radii near 0.2 μm to 0.5 μm, where collision effects begin to substantially reduce the conduction rate.

In a practical LIN soot monitor, excitation might be accomplished by a Nd:Yag laser operating at a wavelength of 1.06 μm, producing a pulse, say, of 1 mJ in 10 ns. Such a pulse focused into a beam with 0.01 cm^2 cross sectional area would heat pure carbon particles to their vaporization temperature near 4500 K. The spectral radiance of incandescent emission from a heated column of spherical particles is given by

$$I_e\left(\frac{\text{watts}}{\text{cm}^2\text{–nm–sr}}\right) = \left[B_\lambda (4500\ K) \right] D_0\, N \int_0^\infty F(r)\, \sigma_a (r)\, dr \tag{3.6-5}$$

Here N is the number density of particles in the volume, and F(r)dr gives the fraction of particles with radii within r and r + dr where the integral of F(r) is unity. We have assumed that the viewed column of soot-bearing gas is optically thin with a laser-excited depth (in the viewed direction) of D_0. The Planck radiation function B_λ (4500 K) gives the emitted light flux normal to a black body surface in watts per square centimeter, nanometer, steradian, at a wavelength of λ (nm). The product of the emitting cross-sectional area of each particle times its emissivity is equated to its absorption cross section, as required by Kirchoff's law.

The absorption cross section is

$$\sigma_a = \frac{4\pi}{3} \rho_c A_A r^3 \tag{3.6-6}$$

Substituting this expression into Eq. (3.6-5) and integrating over r, we find

$$I_e = B_\lambda (4500\ K)\ D_0 A_A \rho \tag{3.6-7}$$

where ρ is the soot mass concentration; i.e.,

$$\rho = \rho_c\, N \int_0^\infty F(r)\, \frac{4\pi r^3}{3}\, dr \tag{3.6-8}$$

This formula can be used to examine the sensitivity of a practical LIN configuration for pure carbon soot. We assume for an example (not optimized system) that the Nd:Yag laser de-

scribed above is used to excite the soot. As illustrated in Figure 3.6-1, its beam is focused into a 0.01 cm^2 cross section to produce the energy density necessary to heat the soot particles to 4500 K. (We assume here that $A_\lambda = 8 m^2/g$ at 1060 nm. If the specific absorption is somewhat smaller, the beam will have to be focused to a commensurately smaller cross section.)

The soot incandescence is observed over a solid angle of 0.1 steradians at right angles to the excitation beam, over the wavelength range from 550 to 600 nm. The geometry, very large spectral separation to the anti-Stokes side, and different time dependences of incident and incandescent light provide extremely strong discrimination against the incident light. We assume that the excited region viewed by the detector has dimensions of 0.1 cm height (H), 1 cm length (L) and 0.1 cm depth (D_0). The Planck function value at 4500 K averaged over 550 to 600 nm is

$$B_{550-600nm}\ (4500\ K) = 0.18\ W/(cm^2\text{–}sr\text{–}nm)$$

The incandescent light power level viewed by the detector is

$$I_D = HL\Delta\lambda\,\Omega\,I_e \tag{3.6-9}$$

where $\Delta\lambda$ and Ω are the wavelength range and observed solid angle mentioned above.

Substituting Eq. (3.6-7) into Eq. (3.6-9), we find

$$I_D = HLD_0 B_\lambda\ (4500\ K)\ \Delta\lambda\,\Omega\,A_\lambda\rho \tag{3.5-10}$$

Thus

$$I_D = \left[7.2 \times 10^{-7}\ \frac{watts\text{–}m^3}{mg}\right]\ \rho \tag{3.6-11}$$

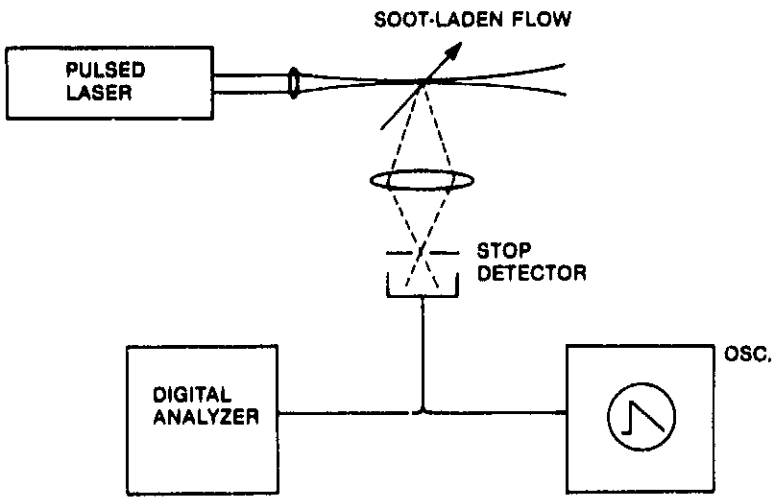

Figure 3.6-1. System configuration for soot measurement by laser-induced incandescence

If this light level is viewed over time increments of 0.1 μs (time resolution necessary to provide the additional measurement of the particle size), the integrated signal is S (joules) = 10^{-7} sec × I_D (watts), or

$$S_I = \left[7.2 \times 10^{-14} \ \frac{\text{Joules}-\text{m}^3}{\text{mg}}\right] \rho \qquad (3.6\text{-}12)$$

Since light pulses at least as small as 10^{-15} joules can be measured accurately using photomultipliers, the indicated sensitivity to pure carbon soot is approximately 0.01 mg/m^3, a concentration which is at least one order of magnitude lower than anticipated in jet engine exhausts.

3.6.3 Potential Problems

While the analysis above indicates the possibility that the LIN technique will provide a signal directly proportional to soot concentration, will give size information, and will be more than sufficiently sensitive, further consideration indicates several problems that would appear to inhibit realization of a robust soot concentration monitor using this technique. Foremost among these problems is the effect caused by volatile adsorbates on the soot particles. Such adsorbates are known to be present, and even sometimes predominate over elemental carbon in diesel exhaust. They are expected to be less prevalent in jet exhaust, but are probably still significant. The effect of these adsorbates is to prevent soot particles from rising to the soot incandescence temperature until the adsorbates have evaporated. At the resultant lower peak temperatures sensitivity is reduced and calibration shifted. These are both serious problems for a robust soot monitor.

A second difficulty relates to the precise control of laser intensity and pulse shape. It is usually difficult to get sufficiently constant intensity across the beam cross section, as well as repeatable pulse shape from a pulsed laser. Controlling laser intensity and pulse shape requires an expensive laser and experienced operator. We have considered the use of CW lasers to reduce the control difficulties noted above. However, sensitivity is seriously compromised in this case, because the illuminated volume must be reduced to get enough power for incandescence.

A third difficulty arises from the possibility of chemical reactions at the heated particle surface, which may change particle cooling rate or produce a chemi-luminescent background.

A fourth difficulty is the dependence of the cooling rate on gas composition, and in particular on the ratio of particle size and molecular mean free path.

3.6.4 Summary

1. Error Sources, expected accuracy, response time, and concentration range.

The LIN technique should have no difficulty meeting the time response and full range capability required for soot concentration measurements. However, the interaction of the numerous physical phenomena and characteristics listed below are sufficiently complex to prevent accurate estimates of individual and aggregate error. The anticipated major error sources are:

a. Nonuniform beam produces uneven heating.

b. Soot partially vaporized before laser pulse termination.

c. Cooling of the soot by evaporation of volatile adsorbates during laser heating delays attainment of vaporization temperature.

d. Chemiluminescence and/or anti-Stokes fluorescence near strongly heated particles becomes significant with respect to thermal emission.

e. Calibration error or changes in calibration.

While possible solutions to each of these problems can be identified, the result is a complex, expensive instrument requiring considerable operator skill to operate accurately. On the other hand, LIN data should be information rich, possibly providing particle sizing and adsorbate load in addition to concentration under well controlled conditions.

2. Principal components

a. Pulsed Nd:Yag laser, 0.1 J/pulse, 10 pps with appropriate beam handling optics.

b. Photomultiplier and optical filter with appropriate optics to collect and filter light from heated region.

c. Fast (0.1 μsec × 100 words) data acquisition system.

d. Microcomputer to analyze pulses, calculate concentration.

e. Calibration system (auxiliary standard such as a filter paper smoke meter, and stable soot source or absolute calibration by standard lamp.)

3. Calibration

A LIN instrument can be calibrated either through an absolute calibration of its receiving optics (using, for example, a standard lamp) or by comparison of its signal to that of a soot measurement standard (such as direct transmission or a filter paper instrument) when both instruments observe the output of a steady soot source. We recommend calibration against a transmission measurement because this procedure should be fastest and most reliable and the LIN instrument should operate at concentrations high enough for a reliable transmission measurement.

4. Significant disadvantages

a. Calibration can depend significantly on laser beam spatial distribution, pulse energy, gas state, and soot adsorbates. Possible variation of these quantities requires frequent recalibration and/or considerable operator skill.

b. Uses high-power lasers requiring good safety control for beam and high voltage.

c. Requires uniform beam with adjustable energy density.

d. Expensive system.

5. Key questions for further study.

a. Intensity of possible chemiluminescence relative to thermal radiation.

b. Possibility of using measurements at two wavelengths to determine particle temperature, which would give a direct measure of the Planck radiation function necessary to calculate the soot concentration. This indication could also be used

to unscramble effect of adsorbates that limit attainment of the particle vaporization temperature. For example, the particle temperature, calculated from the intensity ratio between the two channels, could be determined as a function of laser pulse energy. This approach can be used to adjust the laser pulse energy to that just necessary to raise particle temperature to the vaporization point, so that the carbon particles are not significantly vaporized prior to measurement. An excess energy over calculated values necessary for vaporization ($\approx$ 0.1 J/cm^2) can indicate energy required to evaporate adsorbates, or effects caused by particles substantially larger than 0.1 μm. Chemical reactions at the heated particle surfaces may affect such measurements; this possibility must be evaluated experimentally.

3.7 PHOTOACOUSTIC SPECTROSCOPY (PAS)

3.7.1 General Description

Particulate measurement by photoacoustic spectroscopy (PAS) is based upon the absorption of modulated light by particles suspended in a gas, resulting in sound wave production. Figure 3.7-1 shows a typical system schematic The particles absorb the light that increases the particle temperature. The absorbed heat is transferred rapidly to the surrounding air, increasing local air pressure, and thereby producing a sound wave at the modulation frequency monitored by a microphone. Over a wide range of conditions, the intensity of this sound wave is directly proportional to the gas and particle absorption, providing a measurement of absorption levels too low to be measured directly.

3.7.2 Theoretical Principles

Normally the particle-laden gas is passed through a sample cell along with a modulated light beam (usually provided by a laser). A microphone mounted in the cell wall senses the acoustic signal. If the light modulation frequency is far from the cell's acoustic resonances and acoustic losses by heat conduction and viscosity are neglected, the rms amplitude of the acoustic signal is given by[15]

$$S = \frac{4\,(\gamma - 1)\,\sigma_m}{\sqrt{2}\,\pi\,\omega\,V}\,\frac{b_A}{b_E}\,(1 - e^{-b_E L})\,I_0 \quad . \tag{3.7-1}$$

Here V is the cell volume, L is the cell length along the light beam path, γ is the ratio of specific heats, C_p/C_V, σ_m (mV/Pa) is the microphone sensitivity, ω (rad/sec) is the angular frequency of the modulated light, b_A (m^{-1}) and b_E (m^{-1}) are the absorption and extinction coefficients, and I_0 (watts) is the power of the light source The absorption coefficient, b_A, is

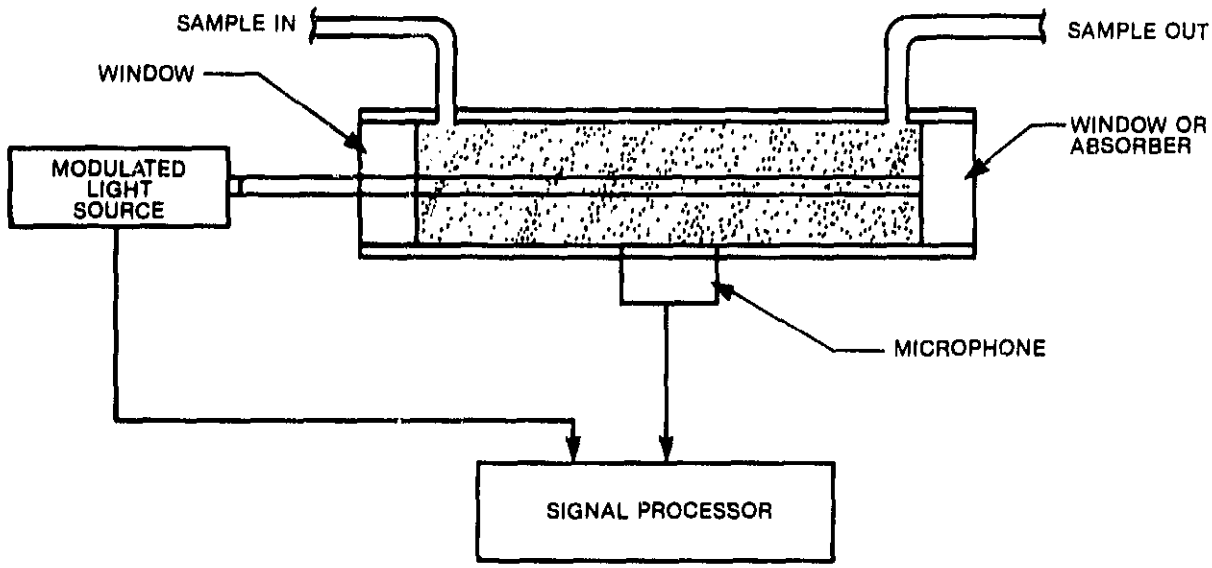

Figure 3.7-1. Schematic diagram of photoacoustic soot measurement instrument

the fraction of the light beam (per unit length) attenuated by particle absorption. The extinction coefficient, b_E, is the fraction of the light beam (per unit length) attenuated by particle absorption and scattering. The signal can be written as

$$S = R \frac{b_A}{b_E} (1 - e^{-b_E L}) \frac{I_0}{L} \tag{3.7-2}$$

where R is the cell responsivity (mv-m/w) given by

$$R = \frac{4 (\gamma - 1) \sigma_m L}{\sqrt{2} \pi \omega V} \tag{3.7-3}$$

When the extinction is small ($b_E L < 1$), Equation (3.7-2) can be further simplified.

$$S = R b_A I_0 \tag{3.7-4}$$

The absorption coefficient can be expressed as $b_A = A_A \rho$, where A_A is the mass specific absorption coefficient (m^2/g) (also called absorption cross section per unit mass) and ρ is the soot mass concentration in the gas (mg / m^3). The mass specific absorption coefficient, A_A, is independent of particle concentration and is a measure of light absorption by a given particle composition and size distribution. The rms signal is then given by

$$S = R A_A \rho I_0 \tag{3.7-5}$$

This relationship is valid for low particle heating, optically thin ($L b_E < 1$) media, a nonresonant cell, and low enough particle loading so that γ = const. The signal is optimized with a cell of small cross sectional area (V/L), low frequency modulation, ω, and a high power light source, I_0. The mass specific absorption, A_A, can depend on the wavelength of the light source.

The PAS system can be operated under two different modes: nonresonant or resonant. At resonance the cell responsivity is increased by the cell quality, Q, according to,[23]

$$R_{res} = QR \tag{3.7-6}$$

Typical values of cell quality are around 100 while values of 800 have been achieved. Both radial and axial modes of resonance have been used. Soot measurements to date have been made in diesel engine exhausts using resonant PAS cells[6,7], but nonresonant cells may ultimately be preferred because Q is sensitive to temperature variations.

Calibrations are required to give accurate values of cell responsivity, R, and the mass specific absorption, A_A. The cell responsivity can be determined reliably by putting an absorbing gas (such as NO_2) of known concentration, ρ_a, and mass specific absorption, A_A into the cell and measuring the microphone signal. The cell responsivity is then

$$R = \frac{S}{A_A \rho_a I_0} \tag{3.7-7}$$

The mass specific absorption coefficient for soot can be predetermined by calibration using gravimetric techniques. As noted previously, this quantity is expected to vary somewhat with

shape, composition, and size distribution of the soot. Values of the specific absorption coefficient are affected, in turn, by the type of combustion source and the sampling method. Resulting difficulties in interpretation of photoacoustic signals are discussed in the next section.

3.7.3 Potential Problems

One difficulty arises in determining an accurate value of A_A for soot. The value of A_A has been found to depend somewhat on the soot particle shape and composition. Soot particles in diesels consist of carbon or graphitic material and 10-70% organic material by weight.[7] The composition of soot particles in gas turbine engines are thought to contain much lower amounts of organics. The organic material in the soot is less absorbent to light than the graphitic material, making the PAS signal very insensitive to the organic fraction. The PAS signal is primarily a measure of the graphitic content of the soot. The organics only become a problem if a gravimetric technique is used with the PAS instrument to determine A_A. Care must be taken to remove the organics prior to weighing so that the measured value of A_A is only due to the carbon content of the soot.

Soot particle shapes vary widely as the particles consist of 0.01 - 0.05 μm carbon building blocks threaded together in lacy agglomerates. The influence of the particle shape on the absorption is still unclear. Originally the absorption was thought to be independent of shape in the Rayleigh regime (particle diameter < light wavelength). Recent calculations[10] indicate that the particle shape can increase the absorption by as much as a factor of 50 even in the Rayleigh regime. The effect of particle shapes in practical engine exhausts on the PAS measurement has not been determined.

PAS detectors of soot in diesel engines have been developed using lasers emitting both visible and invisible light. Faxvog and Roessler[6] first developed a PAS detector for soot using a CO_2 laser operating at $\lambda = 10.6$ μm (see also Osada et al.[24]). With a typical soot diameter of 0.1 μm, the PAS system would be operating in the Rayleigh regime ($d < \lambda$) for the CO_2 wavelength, and the measurement is less dependent on particle size than visible laser systems but more dependent on particle shape.[10] At 10.6 μm, gases in the exhaust (such as CO_2 and H_2O) will absorb some of the radiation, and a dual cell system needs to be used to subtract the signal from the interfering gas. The amplitude and phase response of the two cells must be matched at all times which makes stability difficult to maintain. Also, adjustment of the optics using invisible laser light is more difficult.

PAS detectors of soot using visible light, such as the argon-ion laser ($\lambda = 514.5$, see Japar and Szkarlet[7]), have advantages such as ease of optical alignment, simplicity of one cell operation, and greater sensitivity. Absorption by interfering gases is smaller at $\lambda = 514.5$ nm, and only one cell needs to be used. Sensitivity is greater because the mass specific absorption of carbon at 514.5 nm, is ten times higher than at 10.6 μm wavelength.[10]

Photoacoustic detection may be made under resonant or nonresonant conditions. Japar and Szkarlet[7] used a resonant cell with a quality, $Q = 200$ (see also Japar and Killinger[12]). A resonant cell gives much higher sensitivity than a nonresonant cell but it is difficult to maintain at a constant responsivity. At resonance, the cell responsivity is strongly dependent on the modulation frequency, which must be precisely set. Also, the high flow rates required to make fast response (1 per sec) and the variable gas temperature of engine exhaust can change the resonant frequencies of the cell significantly during operation. For stability, nonresonant operation such as used by Roessler and Faxvog[15] is preferred. The sensitivity is not as good as with resonant operation, but it should be adequate to measure 0.5 mg/m^3 of soot under ideal conditions.

Acoustic isolation of PAS systems measuring soot in diesel engines has been achieved by using high frequency (3-4 kHz) light modulation. Above 1 kHz the acoustic energy spectrum from a reciprocating engine decreases rapidly, so that at 3-4 kHz the background acoustic noise was found to be negligible[6], and PAS measurements have been made using sample lines as short as 1 meter (D. Roessler, private communication, 1983).

Isolating the photoacoustic signal from jet engine noise may be much more difficult. The acoustic rms pressure levels are generally about (10-100) times higher than diesels with a spectrum stronger in the higher frequencies making acoustic isolation much more difficult. To illustrate the problem of the high acoustic background of a jet engine, consider the rms pressure amplitude of the PAS signal, under nonresonant conditions,

$$P_{rms} = S/\sigma_m = \frac{4(\gamma-1)L}{\sqrt{2}\,\pi\omega V} A_A \rho I_0 \qquad (3.7\text{-}8)$$

Now for a cylindrical cell of diameter, D, $L/V = 4/(\pi D^2)$. The angular frequency of modulation is $2\pi f_0$ where f_0 is the chopping frequency; thus

$$P_{rms} = \frac{8(\gamma-1)A_A \rho I_0}{\sqrt{2}\,\pi^3 f_0 D^2} \qquad . \qquad (3.7\text{-}9)$$

For a typical PAS system (D = 0.01 m, f_0 = 500 Hz and I_0 = 1 watt) measuring soot (A_A = 10 m^2 / g) at the lower limit of soot concentration (ρ = 0.5 mg/m^3) the rms pressure level is

$$P_{rms} = 7.3\times10^{-3}\ \text{Pa}$$

In terms of decibels the signal is

$$\text{dB} = 20\ \log_{10} P/P_e = 20\ \log_{10}\left(\frac{7.3\times10^{-3}\ \text{Pa}}{2\times10^{-5}\ \text{Pa}}\right)$$

$$\text{dB} = 51$$

where P_e is the equilibrium rms pressure fluctuation at room temperature and pressure. The near field acoustic levels of a jet engine can be as high as 160 dB. A 60 dB (or 10^{-3}) reduction of the background level to 100 dB is expected because the signal is narrow band ($\approx$ 10 Hz) and the acoustic background is broadband ($\approx$ 10 kHz). The background is still 50 dB above the signal, and reductions by acoustic isolation of 40 dB are difficult to obtain. Operating at the resonance mode will increase P_{rms}, but one expects that the background resonance will increase commensurately. Thus PAS detection of 0.5 mg/m^3 of soot from jet engines may be difficult to obtain without long sample lines and remote detection, which lead to poor response times and sample line bias. Finally, a photoacoustic soot sensor would be expensive as it requires an argon laser ($\approx$\$15,000). The total system with the lock-in amplifier and other equipment could total \$30,000.

3.7.4 Summary

1. Error sources, expected accuracy, response time, and concentration range

   Errors in the PAS determination can derive from a number of sources. The principal error is in the indeterminate organic fraction of the soot and the effect of particle shape on A_A. Values of A_A for the visible region range from 6.1 to 10.8 m^2/g from various combustion sources of soot which is a ± 20% uncertainty in the measurement.[10] For diesel engines (with a relatively narrow range of soot loading), researchers have reported accuracies of ± 15%.

   Background acoustic noise from the jet engine (up to 160 dB) is a serious problem with a technique whose prime detection is acoustic. This problem alone could prevent the PAS measurement of soot without long sample lines and remote detection, which would limit the time response.

   Response times of 0.5-1 second per measurement have been reported for measurements in diesels. Concentration ranges of 0.5 to 200 mg/m^3 of soot from diesels and acetylene flames have been measured using PAS. The lower limit of 0.5 mg/m^3 may be more difficult to obtain in jet engines because of the high acoustic levels (160 dB).

2. Principal components

   The recommended system would consist of a 4 watt, Argon-ion laser, single PAS cell operating in the nonresonant mode, and a light chopper.

   The components are:

   - Argon ion laser
   - Single cell (10 mm × 100 mm volume)
   - Light chopper (up to 1 kHz) and reference photodiode
   - Microphone (hearing aid type)
   - Collimating lens
   - Pump
   - Lock-in amplifier

3. Calibration

   Calibration of the cell consists of two parts. First the cell responsivity is determined by flow of a gas (typically NO_2) of a known absorption and concentration through the cell. Next the mass specific absorption A_A of the soot needs to be determined. Literature values can be used which are accurate to ± 20%. Also A_A can be determined directly by simultaneous gravimetric measurement and PAS detection of the soot. Care must be taken to remove organics and the water content before weighing.

4. Significant disadvantages

   Because of particle shape effects the PAS soot detector has potential inaccuracies, which make the measurement quantitative to ± 15%. The most serious problem is that photoacoustic detection at low concentrations may be prohibitive in the highly acoustic environment of jet engines. Finally the cost of the equipment is expensive (≈$30,000) because the method requies an argon-ion laser along with signal processing equipment.

5. Key questions for further study.

   Effective acoustic isolation techniques need to be investigated and the lower concentration limit of PAS detection determined under a strong acoustic field. These techniques

could be evaluated in an acoustic environment using a commercially available photoacoustic instrument developed for the diesel industry in Japan.[24] The stability of the microphone under high pressure (340 kPa, 50 psi) and high temperature (430 K) needs to be determined.

Section 4

RECOMMENDATIONS FOR FUTURE WORK

The analysis of techniques for soot concentration measurements involves a number of questions whose experimental examination will benefit development of a robust soot sensor. In this section we recommend and document a limited experimental program designed to resolve key questions regarding the instrument concept considered most likely to meet measurement requirements (MODTRAN) and the concept that appears to offer the most information if successful (LIN). A third, commercially developed concept (TEOM) will be used as an auxiliary standard, providing a simultaneous test of its performance. The individual experiments in this program are described below.

1. Improve MODTRAN cell and determine lowest measurable concentrations.

   The original MODTRAN cell used for preliminary experiments was constructed of aluminum. Window vibration was observed to introduce a background signal in this cell that reached an amplitude corresponding to absorption of several percent per meter when the beam was misaligned, so that the window cut off a substantial fraction of it. Several ways to reduce this problem have been proposed and would be tested in this experiment:

   a. Construct cell of heavier material (e.g. brass or lead).

   b. Use larger windows and soft-edged beam.

   c. Size cell so that windows are located at node of wall vibration.

2. Determine effects of higher sample rates (1-5 l/sec) on acoustic field in MODTRAN cell.

   Since the cell volume is several liters (3.2 liters in the present form), sample rates of several liters per second are necessary to achieve one second time response for the measurement system. In this experiment we will map out the acoustic field of the cell as the sample rate is varied from 1-5 l/sec in order to verify that MODTRAN can be operated successfully at high sample rate.

3. Use MODTRAN cell with soot generator to verify performance with soot.

   The MODTRAN instrument will be cross calibrated with TEOM and filter paper instruments. Problems arising from interaction of acoustic field with particle flow will be noted.

4. Identify and test rms pressure sensor capable of stable operation at ambient and elevated temperature and pressure.

   An accurate indication of the fluctuating pressure field is essential for an accurate MODTRAN concentration measurement. The microphone used presently is too delicate for this application. A more rugged, less sensitive pressure sensor will be identified and tested to verify stability over pressure and temperature fluctuations.

5. Test concepts for improved driver that will operate at high temperature and pressure (430 K, 350 kPa).

   A loud speaker is not expected to function as a satisfactory driver far from ambient conditions. Piston and bellows/diaphragm type drivers as well as fluid oscillators will be investigated. The most promising concepts will be tested.

6. Test LIN technique using 1.06 μm Nd:YAG laser and two visible channels for detection to determine feasibility of temperature measurements.

Temperature measurement would provide a direct measure of the Planck function for the soot concentration calculation. Also, temperature measurements would be used to optimize the soot heating. The soot temperature would be measured as a function of the laser pulse energy to determine the minimum energy necessary to reach vaporization. Laser incandescence using this minimum energy would limit temperature errors due to substantial vaporization prior to measurement. Also, excess laser pulse energy over calculated values would indicate volatilization of organic absorbants or effects of particles substantially larger than 0.1 μm. A soot generator would be used to provide steady sample in these experiments.

The LIN technique appears to be difficult to develop as an applied soot concentration sensor in the near term, because little experimental work is available to evaluate and optimize its performance. Nevertheless, this technique is of interest because of the amount of information it may provide, and because it can be used in-situ in flames, as well as in sampled probes. This experiment will provide a revealing test of assumptions used in the LIN analysis, and may point the way to a useful instrument.

Section 5

SUMMARY AND CONCLUSIONS

Rapid response smoke meters with increased range, sensitivity, and accuracy are needed to measure the wide range of smoke emission levels produced by modern commercial and military jet engines. A wide range of particle measurement techniques are surveyed as possible candidate systems. A set of criteria called the General Smoke Meter Requirements describe the ideal characteristics of a practical jet engine smoke meter. These specifications, which would require substantial improvements over existing smoke meter capabilities, include time response (1 per second), range (1-100 mg/m^3), accuracy (0.2 mg/m^3) and particle size range (0.03 to 1.0 μm diameter). The candidate systems are evaluated against these criteria and five of the most promising techniques were chosen for a more in-depth analysis and evaluation. Four of the smoke measurement concepts are optical methods: Modulated Transmission (MODTRAN), Cross Beam Absorption Counter (CBAC), Laser Induced Incandescence (LIN), and Photoacoustic Spectroscopy (PAS). A rapid response filter instrument called a Taper Element Oscillating Microbalance (TEOM) is also evaluated. For each technique the theoretical principles are described, the expected performance is determined, and the advantages and disadvantages are discussed. The expected performance is evaluated against each of the smoke meter specifications, and the key questions for further study are given.

The most promising smoke meter technique analyzed is MODTRAN, which is a variation on a direct transmission measurement. The soot-laden gas is passed through a transmission cell, and the gas pressure is modulated by a speaker. MODTRAN measures only the fluctuating component of the light transmission, which is directly proportional to the light extinction and is insensitive to window contamination and detector variations. Light extinction from soot well below 1% can be measured, lending support to the assumption that soot concentrations down to 1 mg/m^3 can be measured. Direct transmission measurements can be made in the MODTRAN cell both as a cross check and a primary measurement at high soot loadings near 100 mg/m^3. The principal components of MODTRAN are inexpensive. Experimental study of MODTRAN is needed to establish sensitivity limits, to develop a cell driver (speaker) and pressure sensor capable of withstanding high pressure (50 psi, 350 kPa) and temperature (430 K), and to obtain the high flow rates necessary to give 1 reading per second time response.

The remainder of the techniques are rated much lower than MODTRAN. Photoacoustic measurement of soot has been accomplished in diesel engines and is commercially available for diesel applications in Japan. However, the requirements for jet engine soot measurements are much more severe. The most critical problem is detecting the acoustic signal (typically 50 dB for 1 mg/m^3 of soot) in 160 dB of acoustic background. Acoustic shielding of over 110 dB is difficult to obtain, and long sample lines to remove the instrument from the acoustic source limit time response and bias the results.

LIN, which involves heating carbon particles to vaporization and measuring their incandescence, could be the most promising in the long term. It provides a wealth of information (carbon mass concentration to 0.1 mg/m^3, particle size distribution, and volatile fraction), is insensitive to acoustics, and can be used in situ to obtain a spatially resolved measurement. Potential problems due to outgassing of volatile absorbates, surface chemical reactions, and a complex laser system make the technique a subject of further study rather than a method ready for use as a robust soot meter.

TEOM, which is a soot monitor based on filtering and is available as a commercial instrument, will make a good laboratory standard for comparison to other methods, but it is not recommended as a primary smoke meter candidate since it only provides long-time averages.

About 10 seconds is necessary to make a reading at low soot levels (1 mg/m^3), and it is questionable whether the technique can be improved sufficiently to meet the specification of 1 reading per second. Condensation of volatiles and water on the filter and leaks around the ceramic filter are problems that require sample conditioning and careful operation.

CBAC is a single particle counter, measuring the diameter of each particle as it passes through the interference zone created by the crossing of two laser beams. The rms amplitude of the beam attenuation from the carbon particles passing through the interference zone is measured and is directly related to the diameter. The major problem in this single particle counter is that the smallest particles cannot be measured (below 0.05 μm diameter) and the mass of particles below this limit are ignored. Also the CBAC instrument must measure enough particles to obtain a statistically meaningful mass concentration average. The random arrival rate of particles and wide probability distribution of particle diameters make an accurate mass concentration difficult in one second, particularly at low soot loadings of large particles.

Appendix

GENERAL SMOKE METER REQUIREMENTS

1. System inaccuracy must be less than 10% of reading or 0.2 milligrams/cubic meter, whichever is higher, with resolution of 5% of reading. System inaccuracy is defined as the difference, expressed as a percent of the known concentration, between a known mass concentration input and the smoke meter output reading.
2. The system must be capable of meeting the accuracy requirements over a mass concentration range from 1 milligram/cubic meter to 100 milligrams/cubic meter.
3. The system must be capable of meeting the accuracy requirements over a particle size range of from 0.03 micrometers to 1.0 micrometers.
4. The system must be capable of at least 1 mass concentration reading per second assuming a properly conditioned sample is delivered to the instrument input.
5. The system design must allow for digital control of all functions and for digital readout of the system output.
6. The system must be capable of measuring the carbon content of a sample that is 16% water vapor by volume and has a pressure of 350 kPa and a gas temperature of 430 K.
7. The system must have sufficient stability so that accuracy can be maintained with system re-standardization on a one-half hour cycle. The system must have a convenient and reliable standardization system.
8. It is highly desirable that the system be able to differentiate between carbon particles that are smoke and other constituents including gases and non-smoke particles introduced into but not consumed by the combustion process.
9. The system must be packaged so that it can safely operate within specifications while located close to the test vehicle/jet engine in order to maintain short sampling lines. The control may be located in a less severe environment. The expected test cell environmental conditions include:

Temp	255-325 K
Acoustic Noise	160 dB
Vibration	50 micrometers (0-200 Hz)

10. The system should have a reliable calibration method.
11. The system must be reliable and simple to operate and must require a minimum training time for operating technicians.

REFERENCES

[1] "Exhaust Emissions from Gas Turbine Aircraft Turbine Engines," Sub-Council Report, National Industrial Pollution Control Council, February, 1971.

[2] Bahr, D. W., "Control and Reduction of Aircraft Turbine Engine Exhaust Emissions," *Emissions from Continuous Combustion Systems,* W. Cornelius and W. G. Agnew, editors, Plenum Press, New York, 1972.

[3] Naegeli, D. W., and C. A. Moses, "Fuel Microemulsions for Jet Engine Smoke Reduction," J. Eng. Power., Trans. ASME, *105*, pp. 18-23, 1983.

[4] Shaffernocker, W. M., and C. M. Stanforth, "Smoke Measurement Techniques," Air Transportation Meeting, SAE Paper No. 680346, New York, May, 1968.

[5] Aerospace Recommended Practice, ARP 1179A, "Aircraft Gas Turbine Engine Exhaust Smoke Measurement," Society of Automotive Engineers, revised June 1980.

[6] Faxvog, F.R. and D.M. Roessler, "Optoacoustic Measurements of Diesel Particulate Emissions," J. Appl. Physics, *50*, pp. 7880-7882, 1979.

[7] Japar, S.M. and A.C. Szkarlat, "Measurement of Diesel Vehicle Exhaust Particulate Using Photoacoustic Spectroscopy," Comb. Sci. Tech., *24*, pp. 215-219, 1981.

[8] Kerker, M., *The Scattering of Light and Other Electromagnetic Radiation,* Academic Press, New York, 1969.

[9] Kline, S. J. and F. A. McClintock, "Describing Uncertainties in Single-Sample Experiments," Mechanical Engineering, January, 1953.

[10] Roessler, D. M. and F. R. Faxvog, "Optical Properties of Agglomerated Acetylene Smoke Particles at 0.5145-μm and 10.6-μm Wavelengths," J. Opt. Soc. Am., *70*, pp. 230-235, 1980.

[11] Hall, T. C., Jr. and F. E. Blacet, "Separation of the Absorption Spectra of NO_2 and N_2O_4 in the Range of 2400-5000Å," J. Chem. Phys., *20*, pp. 1745-1749, 1952.

[12] Japar, S.M. and D.K. Killinger, "Photoacoustic and Absorption Spectrum of Airborne Carbon Particulate Using a Tunable Dye Laser," Chem. Phys. Lett., *66*, pp. 207-209, 1979.

[13] Melling, A. and J. H. Whitelaw, "Optical and Flow Aspects of Particles," *The Accuracy of Flow Measurements by Laser Doppler Methods,* Proceedings of the LDA-Symposium, P. Buchhave et al., editors, Copenhagen, 1975.

[14] Mazumder, M. K. and K. J. Kirsch, "Flow Tracing Fidelity of Scattering Aerosol in Laser Doppler Velocimetry," Appl. Optics, *14*, p. 894-901, 1975.

[15] Roessler, D.M. and F.R. Faxvog, "Optoacoustic Measurement of Optical Absorption in Acetylene Smoke," J. Opt. Soc. Am., *69*, pp. 1699-1704, 1979.

[16] Wang, J. C. F., H. Patashnick and G. Rupprecht, "A New Real-Time Isokinetic Dust Mass Monitoring System," J. Air Poll. Contr. Assoc., *30*, pp. 1018-1021, 1980.

[17] Wang, J. C. F. and M.A. Libkind, "A Real-Time Particulate Mass Analyzer for Pressurized Fluidized Bed Combustion Exhaust Applications," Sand 82-8829, Sandia National Laboratories, Livermore, CA, November, 1982.

[18] Wang, J. C. F., B. F. Kee, D. W. Linkins and R. W. Lynch, "Real-Time Total Mass Analysis of Particulate in the Stack of an Industrial Power Plant," J. Air Poll. Contr. Assoc., *33*, pp. 1172-1176, 1983.

[19] Whitby, R., R., Gibbs, R. Johnson, B. Hill, S. Shimpi and R. Jorgenson, "Real-Time Diesel Particulate Measurement Using a Tapered Element Oscillating Microbalance," SAE Paper No. 820463, 1982.

[20] Rutter, S., "A Comparison of Techniques for Measuring Particulate Emissions of a Gas Turbine Engine," ASME Joint Power Generation Conference, ASME Paper No. 83-JPGC-GT-14, Indianapolis, IN, September 25-29, 1983.

[21] Ariessohn, P. C. and J. C. F. Wang, "Recent Development of a Real-Time Particulate Mass Sampling System for High Temperature Applications," Sand 83-8867, Sandia National Laboratories, Livermore, CA, March 1984.

[22] Eckbreth, A. C., "Effects of Laser-Modulated Particulate Incandescence on Raman Scattering Diagnostics," J. Appl. Phys., *48*, pp. 4473-4479, 1977.

[23] Rosencwaig, Allan, *Photoacoustic and Photoacoustic Spectroscopy*, Wiley, New York, 1980.

[24] Osada, H., J. Okayama, K. Ishida, O. Saitoh, "Real-Time Measurement of Diesel Particulate Emissions by the PAS Method Using a CO_2 Laser," SAE Paper No. 820461, Detroit, 1982.

1. Report No.	2. Government Accession No.	3. Recipient's Catalog No
NASA CR-168287		

4. Title and Subtitle	5. Report Date
ADVANCED SMOKE METER DEVELOPMENT: SURVEY AND ANALYSIS	November 1984
	6. Performing Organization Code

7. Author(s)	8. Performing Organization Report No.
R. W. Pitz, C. M. Penney, C. M. Stanforth and W. M. Shaffernocker	
	10. Work Unit No. 505-31-52

9. Performing Organization Name and Address	11. Contract or Grant No.
General Electric Company Corporate Research and Development, Schenectady, New York 12301 Aircraft Engine Business Group, Cincinnati, Ohio 45215	NAS3-23532
	13. Type of Report and Period Covered: Final Report

12. Sponsoring Agency Name and Address	14. Sponsoring Agency Code
National Aeronautics and Space Administration 21000 Brookpark Road Cleveland, Ohio 44135	

15. Supplementary Notes

Project Manager, Robert C. Anderson
Fluid Mechanics and Instrumentation Division
NASA Lewis Research Center, Cleveland, Ohio 44135

16. Abstract

Rapid response smoke meters with increased range, sensitivity, and accuracy are needed to measure the wide range of smoke emission levels produced by modern commercial and military jet engines. Ideal smoke meter characteristics are specified to provide a basis for evaluation of candidate systems. After an examination of a wide range of smoke meter concepts, five promising techniques are analyzed in detail to evaluate compliance with the practical smoke meter requirements. Four of the smoke measurement concepts are optical methods: Modulated Transmission (MODTRAN), Cross Beam Absorption Counter (CBAC), Laser Induced Incandescence (LIN), and Photoacoustic Spectroscopy (PAS). A rapid response filter instrument called a Taper Element Oscillating Microbalance (TEOM) was also evaluated. The theory, expected performance, and principal components of each candidate system are described. The most promising smoke meter technique analyzed was MODTRAN which is a variation on a direct transmission measurement where the sample gas pressure is modulated. The analysis indicates that MODTRAN has the potential of making one reading per second over the smoke level range of 1-100 mg/m^3 in the severe environment of a jet engine test cell. Recommendations are made for an experimental program to test the analysis and answer key questions for the two most promising techniques (MODTRAN and LIN).

17. Key Words (Suggested by Author(s))	18. Distribution Statement
Emission, Jet Engine, Smoke, Soot Electro-optical, Measurement, Laser, Instruments	Unclassified-unlimited

19. Security Classif. (of this report)	20. Security Classif. (of this page)	21. No. of Pages	22. Price*
Unclassified	Unclassified	45	

*For sale by the National Technical Information Service, Springfield, Virginia 22161